Journal of Geodynamics 141-142 (2020) 101796, https://doi.org/10.1016/j.jog.2020.101796

New paleomagnetic constraints for the large-scale displacement of the Hronic nappe system of the Central Western Carpathians

Emő Márton[1], Jozef Madzin[2], Dušan Plašienka[3], Jacek Grabowski[4], Jana Bučová[2 5], Roman Aubrecht[2 3] and Marián Putiš[6]

[1] Mining and Geological Survey of Hungary, Paleomagnetic Laboratory, Columbus 17-23, H-1145 Budapest, Hungary; paleo@mbfsz.gov.hu

[2] Earth Science Institute, Slovak Academy of Sciences, Ďumbierska 1, 974 01 Banská Bystrica, Slovakia; jozef.madzin@savba.sk

[3] Department of Geology and Paleontology, Faculty of Natural Sciences, Comenius University, Mlynská dolina, Ilkovičová 6, 842 15 Bratislava, Slovakia; dusan.plasienka@uniba.sk; roman.aubrecht@uniba.sk

[4] Polish Geological Institute – National Research Institute, Paleomagnetic Laboratory, Rakowiecka 4, 00-975 Warsaw, Poland; jgra@pgi.gov.pl

[5] DPP Žilina Ltd, Legionárska 8203, 010 01 Žilina, Slovakia; jana.bucova@gmail.com

[6] Comenius University, Faculty of Natural Sciences, Department of Mineralogy and Petrology, Ilkovičova 6, 842 15 Bratislava, Slovakia; marian.putis@uniba.sk

Abstract

The thin-skinned Hronic nappe system represents the structurally highest tectonic unit in the Late Cretaceous thrust-stack of the Central Western Carpathians. It mostly comprises a Permian volcano-sedimentary sequence and Triassic carbonate sediments which crop out in different parts of the Central Western Carpathians. We carried out a systematic paleomagnetic study on 24 Permian and 20 Triassic localities geographically distributed over 300 km in W-E direction. Several samples from each locality were drilled and oriented in-situ and specimens cut from them subjected to standard paleomagnetic and magnetic mineralogy experiments. The results were evaluated using principal component analysis, statistical evaluation of the characteristic remanences, and applying inclination-only and tilt tests. We documented the pre-tilting age of remanences for the majority of both the Permian and Triassic age groups. However, the latter was interpreted as remagnetized during the Cretaceous Normal Super-Chron in the course of nappe stacking between 90-80 Ma. The Permian group is exhibiting about 70°, the Triassic about 34° clockwise vertical axis rotations with respect to the present north. There is no indication in our data set for oroclinal bending of the Hronic Unit. We interpret the difference in clockwise rotations (about 36°) between Permian and 90-80 Ma as a clockwise block rotation taking place during major extensional and/or compressive events between stable Europe and Africa. Taking into consideration the well-documented counterclockwise rotation observed for the overstep sequences in the Central Western Carpathians and in the Pieniny Klippen Belt, the remagnetization of the Triassic sediments was closely followed by about 94° clockwise rotation. Research in progress will serve to decide if this large clockwise rotation involved the whole Central Carpathian nappe stack or part of this was due to the thin-skinned nappe emplacement of the Hronic Unit.

Key words: Central Western Carpathians, Hronic nappe Unit, Paleomagnetism, Remagnetization, Late Cretaceous, Tectonic rotations

1. Introduction

The Western Carpathians form a northward convex, E-W trending mountain range, which is a part of the European Alpine orogenic system. Based on its structure and tectonic evolution it is divided into three main tectonic zones, namely the External, Central, and Internal Western Carpathians (Plašienka et al., 1997; Froitzheim et al., 2008; Plašienka, 2018). The Central Western Carpathians represent a nappe stack consisting of thick- and thin-skinned nappe units formed and thrust generally to the north-northwest (in recent coordinates) during the Late Cretaceous. The northern and northwestern part of the Central Western Carpathians, lying between the Čertovica thrust-fault and the Pieniny Klippen Belt (Fig. 1), is known as the Tatra-Fatra Belt comprising the Tatric-Fatric-Hronic nappe stack (Plašienka et al., 1997; Plašienka, 2018). The nappe stack is preserved in several fault bounded mega-anticlinal horst structures called the "core mountains" emerging from the sedimentary fill of the surrounding Paleogene and Neogene basins. The uplift of the core mountains, based on zircon and apatite fission-track data (e.g. Burchart 1972; Kováč et al., 1994; Danišík et al., 2004; Králiková et al., 2016), started already in the Paleocene with the rapid acceleration since the Pliocene – Pleistocene.

Most of the published pre-Cenozoic paleomagnetic data from the Central Western Carpathians come from the Fatric Unit, mainly from the Polish part of the Tatry Mts. (Kądziałko-Hofmokl and Kruczyk, 1987; Kruczyk et al., 1992; Grabowski, 1995; 2000; 2005). They are complemented by sporadic data from the Tatric and Hronic units in the Tatry Mts. (Grabowski 1997; 2000; Grabowski et al. 1999; Szaniawski et al., 2012) as well as from the Tatric and Fatric units of the remaining part of the "core mountains": Nízke Tatry, Malá Fatra, Veľká Fatra (Kruczyk et al., 1992; Pruner et al., 1998; Szaniawski et al., 2020), Strážovské vrchy Mts. (Grabowski et al., 2009; Szaniawski et al., 2020) and Malé Karpaty Mts. (Grabowski et al., 2010). The majority of the reported paleomagnetic directions have

been interpreted in terms of early pre- or syn-thrusting remagnetizations acquired during the Cretaceous Normal Super-Chron (Grabowski and Nemčok, 1999; Grabowski, 2000). Exceptions are the Lower Triassic siliciclastic deposits resting directly upon the Tatric crystalline basement (Szaniawski et al., 2012; 2020) and Berriasian pelagic limestones of the Fatric Unit (Grabowski 2005; Grabowski and Pszczółkowski, 2006; Grabowski et al., 2009; 2010) where magnetization has been interpreted as primary. Unlike the Cenozoic paleomagnetic directions showing consistent 50-60° CCW rotations in all principal tectonic units of the Western Carpathians (see comprehensive review by Márton et al., 2016), the pre-Cenozoic paleodirections display a more complex pattern. The distribution of paleodeclinations for the Tatric and Fatric units (both primary and secondary) and their apparent agreement with nappe transport trajectories was originally taken as a proof for oroclinal bending of the Central Western Carpathians or alternatively interpreted in terms of radial thrusting (e.g. Kruczyk et al., 1992). However, recently documented primary magnetizations from the Tatric cover Unit (Szaniawski et al., 2012; 2020) show concordant paleodeclinations relative to the present north, consistent through a considerable part of the Central Western Carpathians, and therefore challenge the oroclinal bending model.

In the Hronic Unit, Late Paleozoic volcanic and sedimentary rocks were the targets of the very early paleomagnetic studies in the Western Carpathians (see review by Krs et al., 1982). Results of these studies were among the first that have been interpreted in terms of large rotations within the Western Carpathians (Kotásek and Krs, 1965; Krs, 1966). The results were originally interpreted as CW vertical axis rotations. Later these paleomagnetic data were reinterpreted as CCW rotations (Márton et al., 1992; Krs et al., 1996), because some doubts had arisen about the sense of rotation in the light of the near-equatorial paleoposition of the studied rocks and the very similar angle of a Cenozoic CCW rotation documented for several areas in the Internal Western Carpathians (Márton et al., 2016 and references therein).

The main aim of the present study was to obtain positive proofs for the sense and amount of rotations in the Hronic Unit. Thus, we conducted a modern paleomagnetic study on the Late Paleozoic volcanic and sedimentary rocks of the basal part of the Hronic Unit (black dots in Fig. 1), on one hand and a new systematic research on the Mesozoic, mostly Triassic sediments of the same unit (Fig. 1). Our research focused on the Nízke Tatry Mts., where the Late Paleozoic and Triassic rocks are well exposed and accessible for sampling. Additionally, we collected samples from the western sector of the Central Western Carpathians (Malé Karpaty, Považský Inovec and Strážovské vrchy Mts.) in order to have a control on possible relative rotations between different partial nappes of the Hronic Unit, which could be attributed to oroclinal bending.

2. Geological background

The structurally lowermost tectonic unit of the Central Western Carpatians is the Tatric Unit. Its more frontal and distal elements, exposed in the Malé Karpaty, Považský Inovec and in the western part of the Malá Fatra Mts. (Fig. 1) are known as the Infra-Tatric Unit (Putiš, 1992; Putiš et al., 2008; Plašienka, 2018). The Tatric and Infra-Tatric units are composed of the Variscan crystalline basement and its Late Paleozoic and Mesozoic para-autochthonous, mostly sedimentary cover. It is overthrust by the thin-skinned Fatric and the uppermost Hronic cover nappe units with Upper Paleozoic to Upper Cretaceous rock sequences. Based on deep reflexion seismic data (Tomek, 1993) the Tatric thrust-sheet is underlain by highly reflective horizons in middle crustal zones. These horizons were interpreted as remnants of the Vahic (South-Penninic) oceanic crust and basement-cover rocks of the Oravic ribbon continent (e.g. Plašienka 1995a; Bielik et al., 2004; Plašienka, 2012; Putiš et al., 2008, 2019) correlative to the Briançonnais units (Tomek, 1993) or Sub-Penninic units of the Western Alps (Schmidt et al., 2008). The Vahic Ocean is considered as the continuation of the Ligurian-Penninic oceanic tract to the Western Carpathians. The only fragments preserved on

the present surface structure in the Western Carpathians interpreted as of the Vahic-Penninic origin are Upper Jurassic to Cretaceous eupelagic sediments and Senonian syn-orogenic clastic deposits of the Belice Unit in the Považský Inovec Mts. (Fig. 1) (Plašienka et al., 1994; Plašienka, 1995b; Plašienka, 2012).

The basal part of the Hronic nappe system is represented by the uppermost Carboniferous-Permian volcano-sedimentary sequence called the Ipoltica Group (Vozárová and Vozár, 1981; 1988). The Ipoltica Group is characterized by the presence of voluminous basic to intermediate volcanic rocks with continental tholeiitic magmatic trend. They are related to a regional extensional tectonic regime, which led to the formation of a rift structure as a part of the continental margin or back-arc settings on the continental crust (Dostal et al., 2003; Vozár et al., 2015).

The Ipoltica Group comprises the uppermost Carboniferous-lowermost Permian Nižná Boca Fm. and the Permian Malužiná Fm. (Fig. 2). The former consists of a regressive lacustrine-deltaic succession including sandy shales, sandstones and conglomerates. The estimated maximum sedimentation age of the Nižná Boca Fm. is younger than 297 Ma, based on SIMS U-Pb detrital zircon dating (Vozárová et al., 2018). Sporadic doleritic sills and dykes, occurring in the upper part of the formation, are regarded as co-magmatic with the main Permian andesitic to basaltic volcanism of the younger Malužiná Fm. (Vozárová and Vozár, 1981; 1988).

The conformably overlying Malužiná Fm. consists of three fining-upward sedimentary megacycles (Vozárová and Vozár, 1981; 1988). These sedimentary cycles are composed of fluvial-lacustrine and alluvial red beds and locally also evaporites. The characteristic feature of the Malužiná Fm. is the extensive andesitic to basaltic volcanism, which was generated during two main eruption phases. The older one belongs to the 1st, the younger and more voluminous one to the 3rd megacycle (Vozár, 1977; 1997; Dostal et al., 2003; Vozár et al.,

2015). The 2nd megacycle consists mainly of fluvial-alluvial clastic rocks with fining-upward trend. Small portions of effusive and volcaniclastic rocks occur at the base of the 2nd megacycle. Uranium mineralization from the middle to upper parts of the 2nd megacycle was dated to 263±11 Ma (Rojkovič, 1997). CHIME dating of detrital monazites from sandstones of the Malužiná Fm. provide the age 280-250 Ma, with the distinct peak at 255 Ma (Vozárová et al., 2014).

A different view on the division of the Malužiná Fm. was published by Novotný and Badár (1971). They suggested that the large volcanic complex is restricted to the Upper Permian. These authors argued that the volcanic bodies, occurring in the lower part of the Malužiná Fm. represent, in fact, hypabyssal rocks genetically associated with the Upper Permian effusive complex.

The Ipoltica Group is directly overlain by Triassic sediments (Fig. 3). The Lower Triassic rocks are represented by siliciclastic deposits, like quartzitic sandstones followed by variegated shales, alternating with marlstones and sandy limestones in the upper part. The Triassic succession is comparatively thick and includes a wide range of carbonates, representing various parts of a shelf environment – from tidal flats and reef platforms up to pelagic intra-shelf basins, which were deposited in two basin and in two carbonate platform sedimentary realms (Havrila, 2011 and references therein). Carbonate sedimentation was interrupted by a fluvial event, at the Carnian-Norian boundary, depositing siliciclastic sediments that flattened basin-platform topography (Lunz Formation, Aubrecht et al., 2017; Kohút et al., 2017). After this event, the unified shallow-water carbonate sedimentation was resumed during the Upper Triassic. The Jurassic and Lower Cretaceous condensed limestones are rare and the youngest sediments of the Hronic Unit are represented by Hauterivian distal turbidites.

Structurally, the Hronic Unit is an internally complicated nappe system with numerous partial nappes and erosional remnants of the original coherent nappe body (Kováč and Havrila, 1998; Havrila, 2011). In the rear (south-eastern parts in the present coordinates), the partial nappes comprise thicker sedimentary sequences involving Late Paleozoic of the Ipoltica Group and Mesozoic rocks. Towards the frontal parts, i.e. to the north and northwest, the partial nappes form a strongly imbricated system built up almost exclusively of carbonate sequences.

The first shortening events in the Hronic Unit is probably manifested by the Hauterivian turbidites. The final, in part gravity-driven emplacement together with the Fatric nappe system over the Tatric units is assumed to be very rapid during the Turonian (Plašienka, 2018). Tectonic transport directions (in present coordinates) vary from the NW-wards in the Nízke Tatry Mts., Chočské vrchy Mts. and Malá Fatra Mts. (Kováč and Havrila, 1998) to W-wards in the Považský Inovec Mts. (Pelech, 2015). Exceptional NE-wards tectonic directions were reported in the internal parts of the Central Western Carpathians, in the Sklené Teplice tectonic window (Hók et al., 2013) and in the SE part of the Tribeč Mts. (Ivanička et al., 1998).

3. Paleomagnetic sampling

Altogether, we collected samples at 24 Late Paleozoic and 20 Mesozoic localities (Figs. 1 to 4). Statistically acceptable directions were obtained for 20 Late Paleozoic (Table 1) and 16 Triassic localities (Table 2). The samples were drilled by using a portable water-cooled gasoline and an electric drill and oriented mainly by a magnetic compass or when the lithology or the situation required (e.g. closeness of a railway line) a sun compass was used. Special care was taken to avoid slumps or weathered material. Localities that failed in retrieving palaeomagnetic directions are listed in Table 3.

Volcanic and sedimentary rocks (red beds) of the Late Paleozoic Ipoltica Group were sampled mainly in the northern part of the Nízke Tatry Mts. in the Ipoltica Valley and parallel valleys (Figs. 1, 2, 4, 5A-C) where the most continuous sections of the Upper Paleozoic rocks are exposed. Additionally, basalts and tuffs were sampled in two quarries in the easternmost part of the Nízke Tatry Mts. and basalts in two quarries (two lava flows in each) in the Malé Karpaty Mts. (Figs. 1, 2, 4A). A doleritic dyke and uppermost Carboniferous to Lower Permian siltstones, close to the dyke, were also sampled at the type locality of the Nižná Boca Fm. in Nižná Boca village.

The Mesozoic rocks were sampled at geographically distributed localities in the Nízke Tatry, Malá Fatra, Strážovské vrchy, Považský Inovec and Malé Karpaty Mts. (Figs. 1, 3, 4). The sampled rocks include Lower Triassic variegated shales (Fig. 5D), Anisian Gutenstein limestones, Upper Anisian-Lower Carnian well-bedded cherty Reifling limestones (Fig. 5E), Lower Carnian Oponitz limestones, the uppermost Carnian-Norian Hauptdolomites and Dachstein Limestones (Fig. 3). Additionally, one locality of Upper Jurassic – Lower Cretaceous pelagic limestones (T19) in the Malé Karpaty Mts. was sampled. The age determination is based mainly on micropaleontology (see comprehensive review by Havrila, 2011).

4. Laboratory methods

The samples were cut to standard-size specimens by a water-cooled wheel-saw. Usually two specimens from a sample were obtained. The natural remanent magnetization (NRM) was measured by using JR-4, JR-5, JR-5A, JR-6A spinner magnetometers in Budapest, Banská Bystrica and Warsaw, respectively. The magnetic susceptibility and anisotropy of the low-field susceptibility was measured by a KLY-2 kappabridge (Agico, Czech Republic). Then, specimens were stepwise demagnetized by either thermal (Schonstedt TSD-1 thermal

demagnetizer and a MMTD28 thermal demagnetizer Magnetic Measurements Ltd., the United Kingdom) or alternating field method (LDA-3A instrument, Agico, Czech Republic and Demag 0179 AF demagnetizer, Technical University, Budapest, Hungary). Magnetic susceptibility was monitored during thermal demagnetization.

Magnetic mineralogy experiments included Currie point measurements (using a CS-3 apparatus combined with a KLY-2 kappabridge, Agico, Czech Republic), acquisition of isothermal remanent magnetization (IRM) and thermal demagnetization of the three-component IRM (Lowrie, 1990). IRM was imparted on selected specimens by using a Molspin pulse magnetizer (maximum field 1 T).

5. Results

5.1. Permian red sediments and igneous rocks

5.1.1. Magnetic mineralogy

Magnetic minerals in these rocks were identified by monitoring the magnetic susceptibility during heating-cooling runs from room temperature up to 700°C. In some cases, the experiments started from liquid nitrogen temperature (e.g. Fig. 6, SMP160, 137).

In most of the basalts, and in intercalated tuffs (Fig. 6, SMP44), the magnetic mineral was identified as a slightly oxidized magnetite with Curie temperature a bit higher than 575°C. Some exhibited the Verwey transition in the low-temperature part of the susceptibility curve (Fig. 6, SMP160), some well-defined Hopkinson peak at 540-580°C (Fig. 6, SMP36). Exception is locality P18, where Curie point temperature around 680°C indicates haematite (Fig. 6, SMP9).

The red shales show presence of haematite, with Curie point around 680°C (Fig. 6, SMP131, 137). In addition, paramagnetic minerals (e.g. iron bearing silicate minerals) must be present

in abundance. The paramagnetic hyperbola was especially well visible on the low-temperature part of the susceptibility curve for sample SMP137 (Fig. 6). The paramagnetic minerals seem to produce magnetite during heating (dramatically increased susceptibility on the cooling curves of SMP131 and SMP137 (Fig. 6).

5.1.2. Paleomagnetic results

The intensity of the NRM signal before demagnetization in the igneous rocks was very variable (1 x 10^{-3} – 5 x 10 A/m) and the magnetic susceptibility was between 245 and 49 229 x 10^{-6} SI. In the red sediments the NRM intensity was in the range of 9 x 10^{-5}– 3 x 10^{-2} A/m, the susceptibility in the range of 37-283 x 10^{-6} SI.

Alternating Field (AF) demagnetization was ineffective for both types of rocks. Stepwise thermal method efficiently demagnetized the NRM signal (e.g. Fig. 7, specimens SMP28, 35, 46, 67, 135A, 156, 228). In cases, where the decay was not complete even at 680°C (Fig. 7, specimens SMP3, 77, 231) the tendency towards the origin of the Zijderveld diagram was clear. Thus, the experiments provided excellent material for principal component analysis (Kirschvink, 1980) and statistical evaluation on the locality level. The results are shown in Table 1. There was only one locality of red sediments where the directions of the NRM did not decay towards the origin, but moved along great circles (locality P3). In this case the McFadden and McElhinny (1988) method was used to determine the locality mean direction, but the result had to be excluded from tectonic interpretations due to larger than 16° confidence circle. It is important to note that the locality mean directions, before tectonic corrections (Table 1), always depart significantly from the direction of the present local Earth´s magnetic field which is a sign of the long-term stability of the paleomagnetic signals.

5.2. Triassic sediments

5.2.1. Magnetic mineralogy

Except for the Lower Triassic variegated siltstone (locality T1), the IRM acquisition curves showed the dominance of a magnetically soft magnetic mineral (Fig. 8). On the thermal demagnetization of the three component IRM, the variegated siltstone (Fig. 8, specimen SMP280B) clearly shows the dominance of the hard and medium hard components, which however, decay parallel to the soft component. The interesting aspect of the variegated siltstone in question is that a substantial part of the NRM survives even 700°C, pointing to hematite as the carrier of the NRM, while the IRM seems to be governed mainly by another magnetic mineral, possibly oxidized magnetite. In the other cases, the largest IRM component was soft. In specimens representing Anisian shallow-water carbonates (Fig. 8, SMP250A) and Anisian – Lower Carnian hemipelagic marly limestones (Fig. 8, SMP540) the soft component decayed well before the Curie point of magnetite, while the susceptibility re-measured after each heating step started to decrease dramatically as soon as the soft component was demagnetized. The IRM acquisition experiments repeated on the same specimens resulted in producing a mineral with much higher than the original intensity.

5.2.2. Paleomagnetic results

Initial values of the NRM were in the 1 x 10^{-3} and in the 1 x 10^{-2} A/m range. Magnetic susceptibilities varied from minus 6 to plus 309 x 10^{-6} SI. Thermal and AF demagnetizations, respectively, of sister specimens from pilot samples served as a basis for choosing the method for demagnetizing the rest of the samples from the respective localities. When the two methods produced similarly well-defined demagnetization curves, AF method was preferred to demagnetize the rest of the samples from a given locality in order to avoid mineralogical changes on heating. However, occasionally AF demagnetization was followed with a single heating step (Fig. 9, SMP 271 and 338A) in order to document that the results of the two methods define the same lines on the Zijderveld diagrams. The curves in Fig. 9 clearly show the presence of two components. The lower temperature component was easily removed and

represents most probably the present day viscous remanent magnetization. The higher-temperature component decayed towards the origin. Exception is specimen SMP280A (Lower Triassic shale), where it was not possible to achieve the complete decay of NRM even at 675°C due to extremely high viscosity, which already started to disturb the measurements at 600°C.

The above results were evaluated by means of principal component analysis (see above) and the components heading towards the origin of the Zijderveld diagrams were entered into the statistical evaluation at the locality level. For locality T1, only a secondary component was identified, which was, however very well-defined for all the collected samples (Table 2, locality T1). The locality mean directions are very well-defined statistically and before tectonic corrections they differ from the present day direction of the Earth´s magnetic field (Dec=0, Inc=60°) at the sampling localities (Table 2).

6. Discussion

6.1. Discussion of the Permian paleomagnetic results

The results represent mostly volcanic rocks (lava flows, dykes, and in one case an intercalated tuff horizon) and red sediments. The positions of the lava flows were possible to measure directly from the attitude of intercalated tuffs or infer from the underlying and/or overlying sediments.

The paleomagnetic directions for the red sediments form two distinct groups (Fig. 10). Both are accompanied by those obtained for igneous rocks of Permian age. The larger group comprises all results from the Boca partial nappe from the Nízke Tatry Mts. and from the Malé Karpaty Mts. The remaining single igneous locality and two sedimentary localities from the Malužiná partial nappe form the other group. When calculating the overall mean paleomagnetic directions for the larger group, before and after tilt corrections, respectively,

we observe some scatter, which is considerably reduced after omitting two directions (Table 1, localities P4, P9) using the method of Vandamme (1994). For the remaining 15 localities the tilt test is positive (Fig. 10) and the overall mean paleomagnetic direction is Dec=249.6°, Inc= -20.4°, k=22.9, α_{95}=8.2. The result is interpreted in terms of about 70° CW net rotation with respect to the present north. It has to be noted, however, that the overwhelming dominance of the reversed polarity magnetizations (except locality P2, close to the bottom of the Ipoltica Valley section) fits better to ages older than 267 Ma for the source rocks (the end of the Kiaman Reverse-polarity Hyperchron is placed at ~ 267 Ma (Menning 1995; Ogg et al., 2016), but this is not critical from the viewpoint of the tectonic interpretation of the paleomagnetic results.

The above overall mean paleomagnetic direction is based on a robust set of data since they represent different lithologies and different carriers of the remanent magnetizations, either haematite (typical for red sediments, but also occurring at locality P18 in a lava flow) or magnetite, typical for the igneous rocks. Moreover, the sampling localities are geographically distributed and the paleomagnetic directions before tilt corrections are far from that of the present Earth´s magnetic field at the sampling area.

The smaller group consisting of localities P15, P16, P17 defines a paleomagnetic direction of Dec=187.4°, Inc=-21.4°, k=84, α_{95}=13.5°, which is an apparently non-rotated paleomagnetic direction (Fig. 10). These localities belong to the Malužiná partial nappe which is structurally in higher position than the Boca partial nappe comprising the other localities from the Nízke Tatry Mts. (Fig. 4B). This result can be considered as the consequence of local tectonics, yet we cannot disregard another option. Namely, that the remanent magnetizations in the Malužiná partial nappe can be much younger than Permian, since before tilt corrections they are close to the reversed polarity counterpart of the direction of the present Earth´s magnetic

field at the sampling area. In any case, at this stage of knowledge we have left them out from the regional tectonic interpretation.

6.2. Discussion of the Triassic paleomagnetic results

The statistically well-defined paleomagnetic directions for the Triassic sediments, mostly carbonates, except locality T1, were subjected to inclination-only as well as tilt tests (Fig. 11, 12). Three localities were not included in the tests. Two of them (T1 and T3) were omitted because of the obviously post-tilting age of the NRM (Fig. 11). For locality T1 the linear segment in the Zijderveld diagram is not decaying towards the origin (Fig. 9, SMP280A), thus the well-defined linear segment must represent secondary NRM. Locality T3 was affected by complicated syn-sedimentary and repeated post-sedimentary tectonic deformations. The third locality excluded from the tests is T9 as a consequence of the Vandamme cutoff (1994). For the remaining 13 localities the tests are positive (Figs.11, 12). Despite of this the primary origin of the magnetizations is not likely. The reason is that the sediments cover the time span from the Anisian to Norian (about 40 Ma) when numerous reversals of the geomagnetic field were detected (Ogg et al., 2016), while the Triassic localities exhibit exclusively normal polarities. Therefore, we interpret the results obtained for the Triassic rocks as the consequence of remagnetization during the Cretaceous Normal Super-Chron. Such interpretation of the new results for the Hronic Unit are in line with previous ones for the Mesozoic rocks of the Fatric and Tatric nappe units. According to Grabowski (2000) and Grabowski et al. (2009), the particular thrust slices were affected by remagnetization during the Cretaceous Normal Super-Chron at various stages of deformation, some in horizontal and some in tectonically inclined position.

A remarkable feature of the assemblage of the tilt corrected locality mean directions, obtained for Triassic rocks from the Hronic Unit is a quite tight cluster close to Dec=34°and Inc=54°.

Although the population of the locality mean directions satisfy the criteria for Fisherian distribution, there are moderate (localities T6, T11-13) or considerable (locality T7) departures from the overall mean declination. As the Triassic results represent different partial nappes, distributed in W-E direction, it is logical to investigate the problem of possible bending after the acquisition of the remanence. As Fig. 13 documents such correlation is not in evidence, which prohibits an interpretation of the declination differences as a result of oroclinal bending or radial thrusting.

The duration of the Cretaceous Normal Super-Chron (124.5-83.5 Ma) leaves quite a long time period for remagnetization. This can be narrowed down to 90-80 Ma, based on numerous fission track and geochronological data. They record a thermal event at 90-80 Ma related to the burial of the crystalline basement due to overthrusting by the cover thin-skinned nappes followed by exhumation and collapse of the overthickened orogenic wedge during the Late Cretaceous to middle Eocene (e.g. for FT data see comprehensive review by Králiková et al., 2016; Putiš et al., 2008; 2019; Etzel et al., 2018).

The temperature in the Tatric-Infra-Tatric crystalline basement had to rise above 320°C, which is the upper limit for the zircon partial annealing zone (Tagami et al., 1998). At the same time the temperature did not exceed 350°C, because the Ar/Ar and Rb/Sr datings of the Tatric crystalline basement mostly record the Late Variscan 320-280 Ma ages (Janák and Onstott, 1993; Maluski et al., 1993; Janák 1994; Kráľ et al., 1997; 2013). There also exist isotope age data directly from the Hronic Unit representing the diagenetic age of tectonically induced burial due to thrusting. This was obtained with K-Ar method on bentonites forming thin layers of pyroclastic material within the Middle Triassic Reifling Fm. in the Tatry Mts. (Sródon et al., 2006) and Považský Inovec Mts. (Wolska et al., 2002) which revealed similar ages around 90-80 Ma. The maximum paleotemperature in sedimentary sequences of the Hronic Unit was estimated to 160-270° C. Colour alteration indices (CAI) in the Hronic Unit

are generally low, pointing only to diagenetic conditions. This elevated temperature is insufficient for thermal resetting (Grabowski et al. 1999; Gawlick et al., 2002), thus the remagnetization in the Triassic sediments is more likely of chemical than thermoviscous origin. The agents for remagnetization can be thrusting expelled orogenic fluids from the Tatric crystalline basement in the Fatric (Grabowski et al., 2009; Prokešová et al., 2012) as well as in the Hronic nappe units.

6.3. Paleotectonic implications

The Permian paleomagnetic inclinations for the Boca partial nappe of the Nízke Tatry Mts. and for the Malé Karpaty Mts. suggest that the Hronic Unit was situated between stable Europe and Africa (Fig. 14). The paleolatitudes for the Triassic rocks fit perfectly the 90-80 Ma interval in a position close to the southern margin of stable Europe, thus reinforcing the acquisition of the remanences during thrusting. Compared to reference stable European and African declinations, a CCW rotation of about 60° taking place after 30 Ma must be taken into account for the Central Western Carpathians (see comprehensive review by Márton et al., 2016). This means that the Hronic Unit must have rotated relative to stable Europe about 90° and to Africa about 110° in CW sense, after 90 Ma (Fig. 14 and supplementary material Table 1). The net vertical axis rotation between the Permian and the Late Cretaceous is about 36° in the CW sense (Table 4). This means about 21° relative to stable Europe and 50° to Africa in the CW sense. The timing of this older rotation is loosely controlled as it must have taken place after the Permian but before 90 Ma. The most likely time is between the Middle Triassic and Middle-Late Jurassic during the opening and closing of the Neo-Tethys Ocean, respectively (e.g. Gawlick and Missoni, 2019). Alternatively, it could be related to the prolonged extensional tectonic regime affecting substantial parts of the Central Western Carpathians during the Jurassic to Early Cretaceous (e.g. Plašienka, 2003; 2018).

According to our new results, the Hronic Unit must have rotated again in the CW sense after 90-80 Ma. This rotation must have been very fast as the final nappe emplacement of the Fatric together with the Hronic Unit over the Tatric Unit took place in a narrow time range during the Turonian (Plašienka, 2018) with the possible continuation to the Santonian in the more external parts (Pelech et al., 2017; Hók et al., 2019). This interpretation is based on the following considerations. The youngest sediments preserved in the Tatric cover unit of the Central Western Carpathians range from the upper Cenomanian (Wolska et al., 2016) to the middle Turonian – Santonian (Pelech et al., 2017 and references therein). This provides the lower age limit for the thrusting of the Fatric and Hronic nappes. The upper age limit is controlled by the oldest coarse-grained deposits of the Gosau Group which are Coniacian in age, regarded as a new post-orogenic sedimentary cycle (Plašienka and Soták, 2015 and references therein). Therefore, the paleomagnetic results from the post-nappe successions of the Gosau Group are of crucial importance to constrain the timing of the CW rotations of the Central Western Carpathian nappes (Grabowski and Nemčok, 1999; Márton et al., 2016). The Gosau Group is represented by wedge-top, piggy-back basins developed on top of the accretionary wedge of the upper plate tip facing the trench/fore-deep depozones of the subducting South-Penninic oceanic or subcontinental crust (for comprehensive review see Plašienka and Soták, 2015; Putiš et al., 2019). The evolution of the Gosau Group basins was largely controlled by the dynamics of the underlying wedge composed of the frontal elements of the Fatric-Hronic nappe systems. The erosional remnants of the originally much more extended Gosau basins in the Central Western Carpathians have been preserved mainly in the northern part of the Malé Karpaty Mts., in the Middle Váh Valley and in the Žilina-Rajec Basin (Plašienka and Soták, 2015). Some other occurrences have been preserved in a zone rimming the southern side of the Pieniny Klippen Belt with complex stratigraphic relations due to the Late Eocene to Miocene tectonics (Fig. 1, 15). So far, only few paleomagnetic

directions of pre-tilting age were published for the Campanian to middle Eocene sediments of the Gosau Group showing large 59-110° CCW vertical axis rotations (Márton et al., 1992; 2013; Túnyi and Márton, 1996). The most reliable result comes from the Campanian red marls in the Malé Karpaty Mts. (Fig. 15, item 1 in Table 1 in Márton et al., 2013) showing about 60° CCW vertical axis rotation, which is in line with evidences for the regional Miocene CCW rotation observed for the External Western Carpathian Flysch Belt, Pieniny Klippen Belt and the Central Carpathian Paleogene Basin (Márton et al., 2016 and references therein). Accordingly, the CW rotations in the Central Western Carpathian cover nappe units should have ceased before the Campanian. Considering the well-documented about 60° CCW general rotation (Márton et al., 2009; 2016) observed for the Late Eocene to Oligocene sediments of the Central Carpathian Paleogene Basin (Fig. 15), which represents the younger overstep sequence with distinctive transgressive position above the Gosau Group in the Žilina-Rajec Basin (Soták et al., 2017; 2019), or more to the east, above various erosional levels of the Central Western Carpathian nappe structure (e.g. Soták et al., 2001) the total pre-Senonian CW rotation inferred is about 94°.

The question is if the post-Cenomanian and pre-Senonian CW vertical axis rotation was entirely or partly due to the emplacement of the Hronic Unit above the deeper nappe units, or the whole assemblage of the Central Western Carpathian nappe pile was participating in it.

The earlier published (see review by Márton et al., 2016) pre-Cenozoic paleomagnetic results from the Central Western Carpathian units (Fig. 15) were obtained at very different times using different field and laboratory methods. Moreover, they produced mostly sporadic data, which are difficult to consider as constraints for tectonic models. Nevertheless, some have been interpreted as a result of oroclinal bending or radial thrusting (e.g. Kruczyk et al., 1992; Grabowski and Nemčok 1999; Grabowski et al., 2010). More recently paleomagnetic results were reported from Lower Triassic red beds resting directly upon the Tatric crystalline

basement (Szaniawski et al., 2012; 2020), which show virtually no rotation in relation to the present north (small black arrows in Fig. 15). Unlike our Permian results, these directions are conspicuously close to the present day Earth´s field direction at the sampling localities before tectonic corrections, yet are interpreted as primary due to positive tilt test. A remarkable feature of these results is that they exhibit consistent paleomagnetic declinations throughout the substantial part of the Central Western Carpathians. Thus, similarly to our present findings, they do not support the oroclinal bending model of the Central Western Carpathians. On the merit of the positive tilt test, Szaniawski et al., (2012; 2020) postulated a post-Lower Triassic moderate CCW rotation with respect to the APWP for stable Europe. These authors assume that this CCW rotation took place during Late Cretaceous thrusting. In the view of our results from the Hronic Unit, this means a considerable relative rotation between the Tatric and Hronic units during the nappe emplacements. Proving or rejecting such model requires further paleomagnetic investigations.

Conclusions

The presented paleomagnetic results from the Late Paleozoic and Triassic rocks of the Hronic nappe units demonstrate that:

1) The Permian overall mean paleomagnetic direction is based on a robust set of data since it relies on locality mean directions, which are geographically distributed, represent different lithologies, and different carriers of the remanent magnetizations. Moreover, the paleomagnetic directions before tilt corrections are far from that of the present Earth´s magnetic field at the sampling area pointing to a long-term stability of the paleomagnetic signal. Tilt test constraining the age of the magnetization is positive. The paleolatitude calculated from the overall mean inclination points to a paleoposition of the studied area close to the European platform during the Permian.

2) The paleomagnetic directions of the Anisian – Norian carbonate sediments are significantly different from that of the present Earth´s magnetic field in the sampling area (evidence for long term stability). Most of the paleomagnetic directions obtained for geographically distributed localities pass inclination-only and tilt tests with the positive result. Nevertheless, the primary origin of the ChRM was excluded because of solely normal polarities and the paleolatitude fitting the 90-80 Ma interval in a position close to stable Europe.

3) The overall mean paleodeclination for the Triassic sediments with Late Cretaceous remagnetizations show about 34° CW rotation relative to the present north, which considering the 60° CCW Miocene rotation of the Central Western Carpathians means about 94° CW vertical axis rotation. This rotation must have taken place during Turonian – Santonian and can be connected to thrusting of the Hronic Unit over the structurally lower nappe units and/or the simultaneous rotation of the whole nappe stack connected to the subduction of the South-Penninic oceanic crust below the Central Western Carpathians accretionary wedge.

4) The older CW rotation affecting the Hronic Unit was about 36°. We interpret it as a vertical axis block rotation connected to major tectonic events in the Neo-Tethys.

5) Our data set does not support oroclinal bending during or after nappe emplacement.

6) Our future research will concentrate on the nappe units below the Hronic Unit, in order to solve problems, like possible simultaneous rotations of the Tatric-Fatric-Hronic nappe stack and the problem of the correct model in which some earlier observed differences in locality mean declinations can be interpreted.

Acknowledgements. This study was financially supported by the National Development and Innovation Office of Hungary (project K128625), the Slovak Research and Development

Agency (projects APVV-0212-12, APVV-17-0170) and VEGA Agency (projects 2/0028/17, 1/0151/19). Constructive reviews by Miguel Garcés and an anonymous reviewer are gratefully acknowledged. We thank Tadeusz Sztyrak for technical assistance in the field and laboratory. Thanks to Tomáš Flajs (National Park Malá Fatra) for working permissions and guidance during field work at localities in the Malá Fatra Mts.

References

Aubrecht, R., Sýkora, M., Uher, P., Li, X.-H., Yang, Y.-H., Putiš, M., Plašienka, D., 2017. Provenance of the Lunz Formation (Carnian) in the Western Carpathians, Slovakia: Heavy mineral study and in situ LA-ICP-MS U-Pb detrital zircon dating. Palaeogeogr. Palaleocl. 471, 233-253.

Bezák, V., Broska, I., Ivanička, J., Reichwalder, P., Vozár, J., Polák, M., Havrila, M., Mello, J., Biely, A., Plašienka, D., Potfaj, M., Konečný, V., Lexa, J., Kaličiak, M., Žec, B., Vass, D., Elečko, M., Janočko, J., Pereszlényi, M., Marko, F., Maglay, J., Pristaš, J. 2004. Tectonic map of Slovak Republic. MŽP SR ŠGÚDŠ, Bratislava.

Bielik, M., Šefara, J., Kováč, M., Bezák, V., Plašienka, D., 2004. The Western Carpathians – interactions of Hercynian and Alpine processes. Tectonophysics 393, 63-86.

Biely, A., Beňuška, P., Bezák, V., Bujnovský, A., Halouzka, R., Ivanička, J., Kohút, M., Klinec, A., Lukáčik, E., Maglay, J., Miko, O., Pulec, M., Putiš, M., Vozár, J., 1992. Geological Map of the Nízke Tatry Mts., 1: 50 000. Geological Institute of Dionýz Štúr, Bratislava.

Burchart, J., 1972. Fission-track age determination of accessory apatite from the Tatra mountains, Poland. Earth Planet. Sc. Lett. 15, 418-422.

Butler, R.F., 1992. Paleomagnetism: Magnetic Domains to Geologic Terranes. Blackwell Scientific Publications. 319 pp.

Danišík, M., Dunkl, I., Putiš, M., Frisch, W., Kráľ, J., 2004. Tertiary burial and exhumation history of basement highs along the NW margin of the Pannonian Basin – an apatite fission track study. Austrian J. Earth Sc. 95/96, 60-70.

Debiche, M.G., Watson, G.S., 1995. Confidence limits and bias correction for estimating angles between directions with applications to paleomagnetism. J. Geophys. Res. 100(B12), 22405-24429.

Dostal, J., Vozár, J., Keppie J. D., Hovorka, D., 2003. Permian volcanism in the Central Western Carpathians (Slovakia): Basin-and-Range type rifting in the southern Laurussian margin. Int. J. Earth Sci. (Geol. Rundsch.) 92, 27-35.

Enkin, R., 2003a. The direction-correction tilt test: an all-purpose tilt/fold test for paleomagnetic studies. Earth Planet. Sc. Lett. 212, 151-166.

Enkin R.J., 2003b. PMGSC Paleomagnetism Data Analysis, v 4.2. Geological Survey of Canada. Sidney B.C., Canada.

Etzel, T.M., Catlos, E.J., Kohút, M., Broska, I., Elliott, B.A., Stockli, D., Miggins, D., O'Brien, T., Tandon, S., Aguilera, K., Yin, Z., 2018. Dating the High Tatra Mountains, Slovakia: Tectonic Implications. Joint 5th Central-European Mineralogical Conference and 7th Mineral Sciences in the Carpathians Conference. Banská Štiavnica, Slovakia, June 26-30. Book of abstracts 20.

Fisher, R.A., 1953. Dispersion on a sphere. Proceedings of the Royal Society of London 217, 295-305.

Froitzheim N., Plašienka D., Schuster R., 2008. Alpine tectonics of the Alps and Western Carpathians. In: McCann T. (Ed.): The Geology of Central Europe. Vol. 2: Mesozoic and Cenozoic. Geol. Soc. Publ. House, London, 1141-1232.

Gawlick, H.J., Havrila, M., Krystyn, L., Lein, R., Mello, J., 2002. Conodont colour alteration indices (CAI) in the Central Western Carpathians and the Northern Calcareous Alps – a comparison. Proceedings of XVII. Congress of Carpathian-Balkan Geological Association Bratislava, September 1-4, 2002., Geol. Carpath., Special Issue 53, 15-17.

Gawlick, H.J., Missoni, S., 2019. Middle-Late Jurassic sedimentary mélange formation related to ophiolite obduction in the Alpine-Carpathian-Dinaridic Mountain Range. Gondwana Res. 74, 144-172.

Grabowski, J., 1995. New paleomagnetic data from the Lower Sub-Tatric radiolarites, Upper Jurassic (Western Tatra Mts). Geol. Q. 39, 61-74.

Grabowski, J., 1997. Paleomagnetic results from the Cover (High Tatric) unit and Nummulitic Eocene in the Tatra Mts (Central West Carpathians, Poland) and their tectonic implications. Annales Societatis. Geologorum Poloniae. 67, 13-23.

Grabowski, J., 2000. Palaeo- and rock magnetism of Mesozoic carbonate rocks in the Sub-Tatric series (Central West Carpathians) – palaeotectonic implications. Polish Geol. Inst., Special Papers, 5, 1-88.

Grabowski, J., 2005. New Berriasian palaeopole from the Central West Carpathians (Tatra Mountains, southern Poland): does it look Apulian? Geophys. J. Int. 161, 1, 65-80.

Grabowski J., Nemčok, M., 1999. Summary of palaeomagnetic data from the Central West Carpathians of Poland and Slovakia: Evidence for the Late Cretaceous – Early Tertiary transpression. Phys. Chem. Earth (A), 24 (8), 681-685.

Grabowski, J., Pszczółkowski A., 2006. Magneto- and biostratigraphy of the Tithonian – Berriasian pelagic sediments in the Tatra Mountains (central Western Carpathians, Poland): sedimentary and rock magnetic changes at the Jurassic/Cretaceous boundary. Cretaceous Res. 27, 398-417.

Grabowski, J., Narkiewicz, K., Poprawa, P., 1999. First results of paleomagnetic and paleothermal (CAI) investigations of the highest Sub-Tatric units in the Polish Tatra Mts. Prz. Geol. 47 (2), 153-158. (in Polish, English summary).

Grabowski, J., Michalík, J., Szaniawski, R., Grotek, I., 2009. Synthrusting remagnetization of the Krížna nappe: high resolution palaeo- and rock magnetic study in the Strážovce section, Strážovské vrchy Mts, Central West Carpathians (Slovakia). Acta Geol. Pol. 59, 2 137-155.

Grabowski, J., Michalík, J., Pszczółkowski, A., Lintnerová, O., 2010. Magneto- and isotope stratigraphy around the Jurassic/Cretaceous boundary in the Vysoká unit (Malé Karpaty Mountains): correlations and tectonic implications. Geol. Carpath. 61, 4, 309-326.

Havrila, M., 2011. Hronicum. Paleogeography and stratigraphy (upper Pelsonian – Tuvalian), deformation and structure. Geol. práce, Spr. 7-103. (in Slovak with English summary).

Hók, J., Pelech, O., Slobodová, Z., 2013. Kinematic analysis of the Veporicum and Hronicum rock complexes within the Sklené Teplice pre-Neovolcanic horst basement (Central Slovakia Neogene volcanic field). Acta Geol. Slov. 5 (2), 129-134

Hók, J., Pelech, O., Teťák, F., Németh, Z., Nagy, A., 2019. Outline of the geology of Slovakia (W. Carpathians). Miner. Slov. 51, 31- 60.

Ivanička, J., Hók, J., Polák, M., Határ, J., Vozár, J., Nagy, A., Fordinál, K., Pristaš, J., Konečný, V., Šimon, L., Kováčik, M., Vozárová, A., Fejdiová, O., Marcin, D., Liščák, P., Macko, A., Lanc, J., Šantavý, J., Szalaiová, V., 1998. Explanations to geological map of the Tríbeč Mts., 1:50 000. Geological Survey of Slovakia, Bratislava, 236p.

Janák, M., 1994. Variscan uplift of the crystalline basement, Tatra Mts, Central Western Carpathians: evidence from 40Ar/39Ar laser probe dating of biotite and P-T-t paths. Geol. Carpath. 45, 293-300.

Janák, M., Onstott, T.C., 1993. Pre-Alpine tectono-thermal evolution of metamorphism in the Tatra Mts., Western Carpathians: P-T paths and 40Ar/39Ar laser probe dating. Terra Abstr., Suppl. 1 to Terra Nova 5, 238.

Kądziałko-Hofmokl, M., Kruczyk, J., 1987. Paleomagnetism of middle-late Jurassic sediments from Poland and implications for the polarity of the geomagnetic field. Tectonophysics 139, 53-66.

Kirschvink, J.L., 1980. The least-squares line and plane and the analysis of palaeomagnetic data. Geophys. J. Res. Astr. Soc. 62, 699-718.

Kráľ, J., Hess, J.C., Kober, B., Lippolt, H.J., 1997. 207Pb/206Pb and 40Ar/39Ar age data from plutonic rocks of the Strážovské vrchy Mts. basement, Western Carpathians. In: Grecula, P., Hovorka, D., Putiš, M. (Eds.), Geological Evolution of the Western Carpathians, Miner. Slovaca-Monograph 253-260.

Kráľ, J., Hók, J., Bachliński, R., Ivanička, J., 2013. Age of diaphtoritic rocks from the Považský Inovec Mts.: Rb-Sr and 40Ar/39Ar mineral data (Western Carpathians). Acta Geol. Slov. 5, 195-210. (in Slovak with English summary).

Kohút, M., Hofmann, M., Havrila, M., Linnemann, U., Havrila, J., 2017. Tracking an upper limit of the "Carnian Crisis" and/or Carnian stage in the Western Carpathians (Slovakia). Int. J. Earth. Sci. (Geol. Rundsch.) 107, 321-335.

Kotásek, J., Krs, M., 1965. Palaeomagnetic study of tectonic rotation in the Carpathian Mountains of Czechoslovakia. Palaeogeogr. Palaeoecl. 1, 39-49.

Kováč, M., Kráľ, J., Márton, E., Plašienka, D., Uher, P., 1994. Alpine uplift history of the Central Western Carpathians: geochronological, paleomagnetic, sedimentary and structural data. Geol. Carpath. 45, 83-96.

Kováč, P., Havrila, M., 1998. Inner structure of Hronicum. Slovak Geol. Mag. 4 (4), 275-280.

Králiková, S., Vojtko, R., Fügenschuh, B., Kováč, M., 2016. Low-temperature constraints on the Alpine thermal evolution of the Western Carpathian basement rock complexes. J. Struct. Geol. 91, 144-160.

Krs, M., 1966. Palaeomagnetic pole position for the Lower Triassic of East Slovakia

(Czechoslovakia). Věstnik, Geological Survey, Prague, XLI, 4, 287-290.

Krs, M., Muška, P., Pagáč, P., 1982. Review of paleomagnetic investigations in the West Carpathians of Czechoslovakia. Geol. práce, Spr. 78, 39-58.

Krs, M., Krsová, M., Pruner, P., 1996. Paleomagnetism and paleogeography of the Western Carpathians from the Permian to the Neogene. In: Morris, A., Tarling, D. H. (Eds), Paleomagnetism and Tectonics of the Mediterranean Region. Geol. Soc. Spec. Publ. 105, 175-184.

Kruczyk, J., Kądziałko-Hofmokl, M., Lefeld, J., Pagáč, P., Túnyi, I., 1992. Paleomagnetism of Jurassic sediments as evidence for oroclinal bending of the Inner West Carpathians. Tectonophysics 206, 315-324.

Lexa, J., Bezák, V., Elečko, M., Mello, J., Polák, M., Potfaj, M., Vozár, J. (Eds.), 2000. Geological map of Western Carpathians and adjacent areas 1:500,000. Bratislava: Ministry of Environment Slovak Republic, Geol. Survey Slovak Republic.

Lowrie, W., 1990. Identification of ferromagnetic minerals in a rock by coercivity and unblocking temperature properties. Geophys. Res. Lett. 17 (2), 159-162.

Maluski, H., Rajlich P., Matte P., 1993. 40Ar-39Ar dating of the Inner Carpathians Variscan basement and Alpine mylonitic overprint. Tectonophysics 223, 313-337.

Márton, E., Pagáč, P., Túnyi, I., 1992. Paleomagnetic investigations on late Cretaceous-Cenozoic sediments from the NW part of the Pannonian Basin. Geol. Carpath. 43, 363-368.

Márton, E., Jeleńska, M., Tokarski, A.K., Soták, J., Kováč, M., Spišiak, J., 2009. Current-independent paleomagnetic declinations in flysch basins: a case study from the Inner Carpathians. Geodin. Acta 22, 73-82.

Márton, E., Grabowski, J., Plašienka, D., Túnyi, I., Krobicki, M., Haas, J., Pethe, M., 2013. New paleomagnetic results from the Upper Cretaceous red marls of the Pieniny Klippen Belt, Western Carpathians: evidence for general CCW rotation and implications for the origin of the structural arc formation. Tectonophysics 592, 1-13.

Márton, E., Grabowski, J., Tokarski, A.K., Túnyi, I., 2016. Palaeomagnetic results from the fold and thrust belt of the Western Carpathians: an overview. In: Pueyo, E. L., Cifelli, F., Sussman, A. J., Oliva-Urcia, B. (Eds), Palaeomagnetism in Fold and Thrust Belts: New Perspectives. Geol. Soc. Spec. Publ. 425, http://doi.org/10.1144/SP425.1.

McFadden, P.L., McElhinny, M.W., 1988. The combined analysis of remagnetization circles and direct observations in paleomagnetism. Earth Planet. Sc. Lett. 87, 161-172.

Menning, M., 1995. A numerical time scale for the Permian and Triassic Periods: An integrative time analysis. In: Scholle, P.A., Peryt, T.M., Ulmer-Scholle, D.S. (Eds.). The Permian of the Northern Pangea. Vol. 1. Springer-Verlag, Berlin, 77-97.

Novotný, L., Badár, J. 1971. Stratigraphy, sedimentology and ore deposits of the late Paleozoic of the Choč Unit in the north-eastern slope of the Nízke Tatry Mts. Miner. Slovaca 3, 23-41 (in Slovak).

Ogg, J.G., Ogg, G.M., Gradstein, F.M., 2016. A concise geologic time scale 2016. Elsevier,

234p.

Pelech, O., 2015. Kinematic analysis of tectonic units of the Považský Inovec Mts. Faculty of Natural Sciences, Comenius University Bratislava, unpublished PhD thesis, 155p.

Pelech, O., Hók, J., Józsa, Š., 2017. Turonian – Santonian sediments in the Tatricum of the Považský Inovec Mts. (Internal Western Carpathians, Slovakia). Austrian J. Earth Sc. 110/1, 21-35.

Plašienka, D., 1995a. Passive and active margin history of the northern Tatricum (Western Carpathians, Slovakia). Geol. Rundsch. 84, 748–760.

Plašienka, D., 1995b. Origin and the structural position of the Upper Cretaceous sediments in the northern part of the Považský Inovec Mts. Part 2: Structural geology and paleotectonic reconstruction. Miner. Slovaca 27, 179-192. (in Slovak with English summary).

Plašienka, D., 2003. Dynamics of Mesozoic pre-orogenic rifting in the Western Carpathians. Mitt. Öster. Geol. Ges. 94, 78-98.

Plašienka, D., 2012. Jurassic syn-rift and Cretaceous syn-orogenic, coarse-grained deposits related to opening and closure of the Vahic (South Penninic) Ocean in the Western Carpathians – an overview. Geol. Q. 56 (4), 601–628.

Plašienka, D., 2018. Continuity and episodicity in the early Alpine tectonic evolution of the Western Carpathians: How large-scale processes are expressed by the Orogenic architecture and rock record data. Tectonics 37, 2029-2079.

Plašienka, D., Soták, J., 2015. Evolution of Late Cretaceous-Palaeogene synorogenic basins in the Pieniny Klippen Belt and adjacent zones (Western Carpathians, Slovakia): Tectonic controls over a growing orogenic wedge. Ann. Soc. Geol. Pol. 85 (1), 43-76.

Plašienka, D., Marschalko, R., Soták, J., Uher, P., Peterčáková, M., 1994. Origin and structural position of Upper Cretaceous sediments in the northern part of the Považský Inovec Mts. Part 1: Lithostratigraphy and sedimentology. Miner. Slovaca 26, 5, 311-334. (in Slovak with English summary).

Plašienka, D., Grecula, P., Putiš, M., Kováč, M., Hovorka, D., 1997. Evolution and structure of the Western Carpathians: An overview. In: P. Grecula, D. Hovorka, M. Putiš (Eds.), Geological evolution of the Western Carpathians: an overview. Miner. Slovaca-Monograph. 1–24.

Polák, M., Plašienka, D., Kohút, M., Putiš, M., Bezák, V., Filo, I., Olšavský, M., Havrila, M., Buček, S., Maglay, J., Elečko, M., Fordinál, K., Nagy, A., Hraško, Ľ., Németh, Z., Ivanička, J., Broska, I., 2011. Geological map of the Malé Karpaty Mts. 1:50 000. MŽP SR – ŠGÚDŠ, Bratislava.

Prokešová, R., Plašienka, D., Milovský, R., 2012. Structural pattern and emplacement mechanisms of the Krížna cover nappe (Central Western Carpathians). Geol. Carpath. 63, 1, 13-32.

Pruner, P., Venhodová, D., Slepičková, J., 1998. Palaeomagnetic and palaeotectonic studies of selected areas of Tatricum, Manín and Krížna units. In: Rakús, M. (ed.) Geodynamic Development of the Western Carpathians. Geological Survey of Slovak Republic, Bratislava, 281-290.

Putiš, M., 1992. Variscan and Alpidic nappe structures of the Western Carpathian crystalline basement. Geol. Carpath. 43 (6), 369-380.

Putiš, M., Gawlick, H.-J., Frisch, W., Sulák, M., 2008. Cretaceous transformation from passive to active continental margin in the Western Carpathians as indicated by the sedimentary record in the Infratatric unit. Inter. J. Earth Sci. 97 (4), 799-819.

Putiš, M., Danišík, M., Siman, P., Nemec, O., Tomek, Č., Ružička, P., 2019. Cretaceous and Eocene tectono-thermal events determined in the Inner Western Carpathians orogenic front Infratatricum. Geol. Q. 63 (2), 248-274.

Rojkovič, I., 1997. Uranium mineralization in Slovakia. Acta Geol. Univers. Comen. Monogr. Bratislava, 117.

Schmid, S.M., Bernoulli, D., Fügenschuh, B., Matenco, L., Schefer, S., Schuster, R., Tschler, M., Ustaszewski, K., 2008. The Alpine-Carpathian-Dinaridic orogenic system: correlation and evolution of tectonic units. Swiss J. Geosci. 101, 1, 139-183.

Schwartz, S.Y., Van der Voo, R., 1983. Paleomagnetic evolution of the orocline hypothesis in the central and southern Appalachians. Geophys. Res. Lett. 10, 505-508.

Soták, J., Pereszlenyi, M., Marschalko, R., Milička, J., Starek, D., 2001. Sedimentology and hydrocarbon habitat of the submarine-fan deposits of the Central Carpathian Paleogene Basin (NE Slovakia). Mar. Petrol. Geol. 18, 87–114.

Soták, J., Pulišová, Z., Plašienka, D., Šimonová, V., 2017. Stratigraphic and tectonic control of deep-water scarp accumulation in Paleogene synorogenic basins: a case study of the Súľov Conglomerates (Middle Váh Valley, Western Carpathians). Geol. Carpath. 68, 5, 403-418.

Soták, J., Kováč, M., Plašienka, D., Vojtko, R., 2019. Orogenic wedging and basin formation in the Central Western Carpathians: New insights from Súľov–Domaniža and Žilina–Rajec basins. In: Broska, I., Kohút, M. & Tomašových, A. (eds.): Proceedings of the Geologica Carpathica 70 Conference, Earth Science Institute of the Slovak Academy of Sciences, Bratislava 2019, 43-44, ISBN 978-80-85754-42-1.

Speranza, F., Sagnotti, L., Mattei, M., 1997. Tectonics of the Umbria-Marche-Romagna Arc (central northern Apennines, Italy). J. Geophys. Res. 102 B2, 3153-3166.

Szaniawski, R., Ludwiniak, M., Rubinkiewicz, J., 2012. Minor counterclockwise rotation of the Tatra Mountains (Central Western Carpathians) as derived from paleomagnetic results archieved in hematite-bearing Lower Triassic sandstones. Tectonophysics, 560-561, 51-61.

Szaniawski, R., Ludwiniak, M., Mazzoli, S., Szczygieł, J., Jankowski, L., 2020. Paleomagnetic and magnetic fabric data from Lower Triassic red beds of the Central Western Carpathians: New constraints on the paleogeographic and tectonic evolution of the Carpathian region. J. Geol. Soc. 177, 509-522.

Środoń, J., Kotarba, M., Biroň, A., Such, P., Clauer, N., Wójtowicz A., 2006. Diagenetic history of the Podhale-Orava Basin and the underlaying Tatra sedimentary structural units (Western Carpathians): evidence from XDR and K-Ar of illite smectite. Clay Miner. 41, 75-774.

Tagami, T., Galbraith, R.F., Yamada, R., Laslett, G.M., 1998. Revised annealing kinetics of

fission tracks in zircon and geological implications. In: Van den Haute P., De Corte F. (Eds.), Advances in fission-track geochronology. Kluwer Academic Publishers, Dordrecht, 99-112.

Tomek, Č., 1993. Deep crustal structure beneath the central and inner West Carpathians. Tectonophysics 226, 417-431.

Torsvik, T.H., Van der Voo, R., Preeden U., Mac Niocaill, C., Steinberger, B., Doubrovine, P.V., van Hinsbergen, D.J.J., Domeier, M., Gaina, C., Tohver, E., Meert, J.G., McCausland, P.J.J., Cocks, L.R.M., 2012. Phanerozoic polar wander, palaeogeography and dynamics. Earth Sci. Rev. 114, 325-368.

Túnyi, I., Márton, E., 1996. Indications for large Tertiary rotation in the Carpathian–Northern Pannonian region outside the North Hungarian Paleogene Basin. Geol. Carpath. 47, 43-49.

Vandamme, D., 1994. A new method to determine paleosecular variation. Phys. Earth Planet. Inter. 85, 131-142.

Vozár, J., 1977. Magmatic rocks of the tholeiite series in the Permian of the Choč nappe in the West Carpathians. Miner. Slovaca 9 (4), 241-258. (in Slovak with English summary).

Vozár, J., 1997. Rift-related volcanics in the Permian of the Western Carpathians. In: Grecula, P., Hovorka, D., Putiš, M. (Eds.), Geological evolution of the Western Carpathians. Miner. Slovaca-Monograph. 225-234.

Vozár, J., Spišiak, J., Vozárová, A., Bazarnik, J., Kráľ, J., 2015. Geochemistry and Sr, Nd isotopic composition of the Hronic Upper Paleozoic basic rocks (Western Carpathians, Slovakia). Geol. Carpath. 66 (1), 3-17.

Vozárová, A., Vozár, J., 1981. Lithostratigraphical characteristics of the late Paleozoic of the Hronic Unit. Miner. Slovaca 13 (5), 385-403. (in Slovak).

Vozárová, A., Vozár, J., 1988. Late Paleozoic in the Western Carpathians. GÚDŠ, Bratislava, 314 p.

Vozárová, A., Konečný, P., Vďačný, M., Vozár, J., Šarinová, K., 2014: Provenance of Permian Malužiná Formation sandstones (Hronicum, Western Carpathians): evidence from monazite geochronology. Geol. Carpath. 65 (5), 329-338.

Vozárová, A., Larionov, A., Šarinová, K., Vďačný, M., Lepekhina, E., Vozár, J., Ľvov, P., 2018. Detrital zircons from the Hronicum Carboniferous-Permian sandstones (Western Carpathians, Slovakia): depositional age and provenance. Int. J. Earth Sci. (Geol. Rundsch.), 107, 1539-1555.

Wolska, A., Szulc, J., Koszowska, E. 2002. K/Ar dating of the Middle Triassic tuffs from the Central Carpathians and its paleotectonic context. In: Michalík, J. Hudáčková, N., Chalupová, B., Starek, D. Paleogeographical, Paleoecological, Paleoclimatical developments of Central Europe. ESSEWECA 5-7th June, 2002, Bratislava, Abstract Book, 73-74.

Wolska, A., Bąk, K., Bąk, M., 2016. Siliciclastic input into Upper Cenomanian synorogenic sediments of the High-Tatric Unit, Central Western Carpathians (Tatra Mountains); petrography, geochemistry and provenance. Geol. Q. 60 (4), 919-934.

Table 1

	Locality	Litostratigraphy	Coordinates	n/no	D°	I°	K	α_{95}°	D_C°	I_C°	k	α_{95}°	Dip	Lat°	Lon°	δp°	δm°	B95°	plat°
NT																			
P1	Ipoltica 2 SMP128-137	Malužiná Fm. red shale 1st megacycle Lower Permian	48°58'17.1" 19°58'54.9"	10/10	249	-23	230.2	3.2	241	-12.2	230.2	3.2	358/27	23.5	128.4	3.2	1.6	2.3	6.2
P2	Ipoltica 3 SMP138-147	Malužiná Fm. basaltic andesite/basalt 1st megacycle Lower Permian	48°58'16.0" 19°58'54.9"	10/10	97.1	12.3	72.3	5.7	90.4	15.1	72.3	5.7	358/27	5.5	104.6	5.9	3.0	4.2	7.7
P4a	Ipoltica 5a SMP180-190	Malužiná Fm. basaltic andesite/basalt 1st megacycle Lower Permian	48°58'33.8" 19°58'41.0"	9/11	45.0	-22.0	37.7	8.5	73.1	-42.1	37.7	8.5	353/46						
P5	Ipoltica 7 SMP213-218	Malužiná Fm. red siltstone 1st megacycle Lower Permian	48°58'50.6" 19°58'30.4"	5/6	268.4	-10.9	52.7	10.6	258.1	-12.8	52.7	10.6	351/46	12.7	114.7	10.8	5.5	7.7	6.5
P6	Ipoltica 4 SMP148-160	Malužiná Fm. basaltic andesite/basalt 3rd megacycle Upper Permian	48°59'42.9" 19°57'42.2"	12/13	250.1	-17.4	42.7	6.7	242.2	-10.2	42.7	6.7	348/32	22.1	128.2	6.8	3.5	4.8	5.3
P7	Ipoltica 1 SMP100-108	Malužiná Fm. basaltic andesite/basalt 3rd megacycle Upper Permian	49°00'04.6" 19°57'16.0"	9/9	273.5	-14.2	279.9	3.1	267	-10.0	279.9	3.1	8/30	5.8	108.9	3.1	1.6	2.2	5.0
P8	Nižný Chmelinec SMP259-266	Malužiná Fm. basaltic andesite/basalt 3rd megacycle Upper Permian	48°58'35.7" 19°54'04.0"	5/8	261.4	-12.3	90.7	8.1	248.2	-27.6	90.7	8.1	322/38	25.3	116.6	8.8	4.8	6.5	14.6
P9	Svarinka 4 SMP233-240	Malužiná Fm. basaltic andesite/basalt 3rd megacycle Upper Permian	48°58'31.5" 19°52'06.9"	8/8	241.3	13.6	54.9	7.5	256.6	+22.7	54.9	7.5	350/45						
P10	Svarinka 2-3 SMP228-232	Malužiná Fm. red shale/siltstone + basaltic andesite/basalt 3rd megacycle Upper Permian	48°50'41.2" 19°51'53.1"	5/5	250.3	-17.9	138.1	6.5	241.4	-10.3	138.1	6.5	348/35	22.4	128.8	6.6	3.4	4.7	5.2
P11	Kvetnica 1 SMP30-39 SMP47-50	Malužiná Fm. basaltic andesite/basalt 3rd megacycle Upper Permian	49°00'38.8" 20°17'14.2"	9/14	249.2	-41.2	62.3	6.6	247.8	-15.3	62.3	6.6	63/26	20.4	122.2	6.8	3.5	4.9	7.8
P12	Kvetnica 2 SMP40-46	Malužiná Fm. tuffs 3rd megacycle Upper Permian	49°00'38.8" 20°17'14.2"	7/7	266.3	-50.5	165.2	4.7	259.2	-25.9	165.2	4.7	63/26	17.3	109.2	5.1	2.8	3.7	13.6
P13	Nižná Boca 1 SM2418-2425	Nižná Boca Fm. doleritic dyke Upper Permian?	48°56'59.5" 19°46'00.3"	8/8	282.6	-38.0	80.9	6.2	220.3	-40.2	80.9	6.2	340/65	49.0	134.5	7.5	4.5	5.8	22.9

Table 1 continuation

	Locality	Litostratigraphy	Coordinates	n/no	D°	I°	K	α_{95}°	D_C°	I_C°	k	α_{95}°	Dip	Lat°	Lon°	δp°	δm°	B95°	plat°
P14	Nižná Boca 2 SM2426-2434	Nižná Boca Fm. siltstone Upper Permian?	48°56'59.5" 19°46'00.3"	8/9	271.7	-34.3	55.5	7.5	223.6	-31.0	55.5	7.5	340/65	42.3	136.6	8.4	4.7	6.3	16.7
P15	Malužiná quarry SMP51-75	Malužiná Fm. basaltic andesite/basalt 3rd megacycle Upper Permian	48°58'29.6" 19°45'21.5"	16/25	217.7	-72.3	86.8	4.0	191.9	-25.3	86.8	4.0	360/50	53.0	180.3	4.3	2.3	3.2	13.3
P16	Malužiná forest 1 SMP76-87	Malužiná Fm. red siltstone 3rd megacycle Upper Permian	48°58'42.8" 19°46'45.5"	10/12	204.3	-52.3	31.2	8.8	178.9	-23.8	31.2	8.8	323/41	53.4	201.6	9.4	5.0	6.9	12.4
P17	Malužiná forest 2 SMP88-99	Malužiná Fm. red siltstone 3rd megacycle Upper Permian	48°58'42.8" 19°46'45.5"	10/12	209.0	-38.0	29.1	9.1	191.1	-14.7	29.1	9.1	323/41	47.5	183.4	9.3	4.8	6.7	7.5
MK Mts.																			
P18	Sološnica 1 SMP1-21	Malužiná Fm. basaltic andesite/basalt 3rd megacycle Upper Permian	48°26'43.1" 17°13'17.6"	13/21	280.0	7.0	126.7	3.7	268.3	-25.1	126.7	3.7	340/70	10.9	99.6	4.0	2.1	2.9	13.2
P19	Sološnica 2 SMP109-118	Malužiná Fm. basaltic andesite/basalt 3rd megacycle Upper Permian	48°26'43.1" 17°13'17.6"	9/10	272.8	-24.6	79.7	5.8	232.1	-28.3	79.7	5.8	340/70	36.0	126.8	6.4	3.5	4.7	15.1
P20	Lošonec 1 SMP22-29	Malužiná Fm. basaltic andesite/basalt 3rd megacycle Upper Permian	48°29'23.5" 17°22'15.7"	6/8	259.7	16.5	41.7	10.5	261.7	-14.1	41.7	10.5	333/84	10.9	108.8	10.7	5.5	7.7	7.2
P21	Lošonec 2 SMP119 127	Malužiná Fm. basaltic andesite/basalt 3rd megacycle Upper Permian	48°29'23.5" 17°22'15.7"	10/9	262.7	7.9	146.5	4.0	253.4	-18.5	146.5	4.0	333/84	18.1	113.5	4.2	2.2	3.0	9.5

Table 1: Hronic Unit, Late Paleozoic Ipoltica Group, characteristic remanence magnetizations. Summary of locality/site mean paleomagnetic directions based on the results of principal component analysis (Kirschvink, 1980). Localities are numbered according to the Fig. 1 and 4. Key: geographic coordinates (WGS84) measured by GPS, n/no: number of used/collected samples (the samples are independently oriented cores); D, I (D_c, I_c): declination, inclination before (after) tilt correction; k and α_{95}: statistical parameters (Fisher, 1953). Lat and Lon: coordinates of the paleomagnetic pole; δm and δp: half cones of the error ellipse of the paleomagnetic pole. Plat: paleolatitude. References for geological ages: Vozárová and Vozár 1981, 1988, Vozárová et al. 2014, 2018.

Table 2

	Locality	Litostratigraphy	Coordinates	n/no	D°	I°	k	α_{95}°	D_C°	I_C°	k	α_{95}°	dip	remark	Mts	Lat °	Lon°	δp°	δm°	B95°	plat°
T1	Šuňava SMP279-287	Šuňava Beds Lower Triassic	49°01'01.0" 20°01'56.2"	9/9	66.2	42.3	30.4	9.5	54.4	21.1	30.4	9.5	15/30	postfolding	NT						24.5
T2	Liptovské Revúce SMP311-316	Gutenstein Fm. Anisian	48°54'15.8" 19°10'05.6"	6/6	140.5	71.4	51.0	9.5	28.9	48.9	51.0	9.5	8/52		VF	60.9	139.5	12.5	8.2	10.1	29.8
T3	Podbrezová-Lopej SMP337-348	Gutenstein Fm. Anisian	48°49'11.1" 19°29'50.7"	10/12	44.4	46.4	185.0	3.6	20.8	12.8	185.0	3.6	342/50	postfolding	NT						27.7
T4	Svarínka 6 SMP247-258	Gutenstein Fm. Anisian	49°00'00.5" 19°51'06.7"	10/12	77.3	24.7	49.5	7.2	27.4	51.9	49.5	7.2	300/60		NT	63.8	138.5	9.8	6.7	8.1	32.5
T5	Stará Lehota SMP635-645	Gutenstein Fm. Anisian	48°38'23.5" 17°56'00.1"	7/11	65.8	19.8	62.9	7.7	19.1	53.4	62.9	7.7	285/62		PI	69.6	146.9	10.7	7.4	8.9	34.0
T6	Homôľka SMP536-548	Reifling Fm. Upper Anisian – Lower Carnian	48°54'28.8" 18°14'14.4"	9/12	89.6	56.0	223.6	3.5	52.7	71.7	223.6	3.5	301/23		SV	58.0	74.2	6,1	5.3	5.7	56.5
T7	Dolný Jelenec SMP317-325	Reifling Fm. Upper Anisian – Lower Carnian	48°51'32.9" 19°09'19.6"	8/9	279.0	79.0	42.1	8.6	357.4	35.6	42.1	8.6	11/54		VF	60.8	204.2	10.0	5.8	7.6	19.7
T8	Zámostie SMP326-336	Reifling Fm. Upper Anisian – Lower Carnian	48°49'31.8" 19°26'07.2"	11/11	63.0	64.0	203.8	3.2	39.0	44.9	203.8	3.2	9/25		NT	52.5	131.6	4.0	2.6	3.2	26.5
T9	Michalovo SMP376-386	Reifling Fm. Upper Anisian – Lower Carnian	49°00'05.7" 19°44'15.8"	11/11	90.8	61.3	267.5	2.8	132.4	71.2	267.5	2.9	229/20	Vandamme cutoff	NT						
T10	Liptovská Porúbka SMP399-417	Reifling Fm. Upper Anisian – Lower Carnian	49°01'00.2" 19°43'00.4"	8/20	23.0	7.1	61.4	7.1	24.6	57.1	61.4	7.1	201/50		NT	69.0	133.0	10.4	7.6	8.9	37.7
T11	Svarín SMP364-375	Reifling Fm. Upper Anisian – Lower Carnian	49°00'45.7" 19°51'37.4"	11/12	126.3	40.1	57.5	6.1	62.0	67.0	67.0	5.6	337/53 37/45		NT	50.8	84.5	9.3	7.7	8.5	49.7
T12	Východná SMP387-397	Reifling Fm. Upper Anisian – Lower Carnian	49°02'36.2" 19°53'09.3"	11/11	92.0	40.0	59.7	6.0	63.6	60.1	59.7	6.0	308/30		NT	45.7	95.2	9.1	6.9	7.9	41.0
T13	Važec SMP267-278	Reifling Fm. Upper Anisian – Lower Carnian	49°03'32.3" 19°57'21.6"	11/12	99.8	70.9	35.4	7.8	84.9	49.8	27.1	8.9	60/22 94/23 84/20		NT	25.8	92.1	11.9	7,9	9.7	30.6
T14	Liptovská Osada SMP197-206	Wetterstein Fm. Lower Anisian – Upper Carnian	48°56'25.8" 19°15'48.0"	6/9	34.4	58.1	352.2	3.6	25.2	37.6	352.2	3.6	8/22		VF	55.6	154.5	4.2	2.5	3.2	21.1
T15	Podbrezová-Piesok SMP349-363	Oponitz Beds Lower Carnian	48°49'12.4" 19°33'36.1"	11/13	123.8	83.4 82.4	38.2	7.5	17.6	63.2	38.2	7.5	3/30		NT	77.3	121.9	11.8	9.3	10.5	44.7
T16	Liptovský Hrádok SMP161-172	Hauptdolomite Fm. uppermost Carnian - Norian	49°02'39.1" 19°43'55.4"	12/12	54.8	67.3	175.6	3.3	38.9	37.2	175.6	3.3	25/32		NT	48.2	138.1	3.9	2.3	2.9	20.8

Table 2. Hronic Unit, Triassic sediments, characteristic remanence magnetizations. Summary of locality mean paleomagnetic directions based on the results of principal component analysis (Kirschvink, 1980). Localities are numbered according to Fig. 1 and 4. Key: geographic coordinates (WGS84) measured by GPS, n/no: number of used/collected samples (the samples are independently oriented cores); D, I (D_c, I_c): declination, inclination before (after) tilt

correction; k and α_{95}: statistical parameters (Fisher, 1953). Lat and Lon: coordinates of the paleomagnetic pole; δm and δp: half cones of the error ellipse of the paleomagnetic pole. plat: paleolatitude. References for geological ages: Havrila 2011.

Table 3

	Locality	Litostratigraphy	Coordinates	remark	dip	Mts.
P3	Ipoltica 6 SMP191-196	Malužiná Fm. red siltstone/sandstone 1st megacycle Lower Permian	48°58'16.0" 19°58'54.9"	α_{95}=20	22/40	NT
P4b	Ipoltica 5b SMP207-212	Malužiná Fm. basaltic andesite/basalt 1st megacycle Lower Permian	48° 58'33.8" 19° 58'41.1"	α_{95}=31	353/46	NT
P22	Spišské Bystré SMP173-179	Malužiná Fm. basaltic andesite/basalt 3rd megacycle Upper Permian	49°01'39.1" 20°15'28.9"	unstable	9/30	NT
P23	Svarínka 1 SMP219-227	Malužiná Fm. basaltic andesite/basalt 3rd megacycle Upper Permian	48°58'41.2" 19°51'53.1"	heavily overprinted and becomes unstable before complete demagnetization	337/34	NT
P24	Svarínka 5 SMP241-246	Malužiná Fm. red shale 3rd megacycle Upper Permian	49°58'31.5" 19°52'06.9"	about 30% of the original intensity is lost by 675°, before that large scatter, at 675° instability sets in	344/42	NT
T17	Terchová SMP831-842	Reifling Fm. Upper Anisian – Lower Carnian	49°14'54.7" 19°02'20.3"	enormous scatter	5/34	MF
T18	Ježovka SMP656-669	Dachstein Fm. Carnian - Norian	49°31'53.0" 17°20'42.0"	well-defined specimen directions exhibit great circle distribution	334/52	MK
T19	Chteľnica 1 SMP646-651	Upper Jurassic - Lower Cretaceous	49°35'51.9" 17°36'18.6"	two population of directions	360/50	MK
T20	Chteľnica 2 SMP652-655	Dachstein Fm. Carnian - Norian	49°35'51.9" 17°36'18.6"	heavily overprinted/weak remanence	358/48	MK

Table 3. Rejected localities. For the location see Fig. 1, 4. NT=Nízke Tatry Mts., MF=Malá Fatra Mts., MK=Malé Karpaty Mts.

Table 4

												Based on localities				Based on samples			
Area	Age	N	D°	I°	k	α_{95}°	D_c°	I_c°	k	α_{95}°	fold test	Pole lat°	Pole long°	K	A95°	Pole lat°	Pole long°	K	A95°
Hronic Unit	Triassic	13	74.3	59.0	6.4	17.8	34.4	54.3	20.1	9.5	positive 85±24%	61.3	122.2	13.6	11.7	60.3	118.2	11.1	4.0
Hronic Unit	Permian	15	85.0	18.0	14.3	10.5	69.6	20.4	22.9	8.2	positive 82±49%	21.7	117.9	24.8	7.8	21.4	117.3	21.2	2.8

Table 4. Overall mean palaeomagnetic directions and overall mean palaeomagnetic poles for the Hronic Unit.
Key: N: number of geographically distributed localities; D°, I° and D_C°, I_C°: declination, inclination before and after tilt correction; k, α_{95}° and K, A95° statistical parameters (Fisher, 1953) of the palaeomagnetic directions and palaeomagnetic poles, respectively. Tilt test based on Enkin (2003a).

Supplementary Table 1

	stable Europe				Africa				Hronic Unit				stable Europe – Hronic Unit		Africa – Hronic Unit	
	N	Pole lat.	Pole lon.	A95	N	Pole lat. N	Pole lon. E	A95	N	Pole lat.	Pole lon.	A95	Poleward displacement	Apparent rotation	Poleward displacement	Apparent rotation
30 Ma	2	80.3	152.6	21.1	8	82.6	173.6	6.0	10	46.5	296.6	7.3	4.8 ± 8.5	-68.4 ±21.8	5.0 ±6.9	-63.2 ±9.0
90 Ma	4	73.4	158.1	6.2	20	70.3	238.0	2.6	13	61.3	122.2	11.7	-0.8 ± 9.4	22.1 ±12.0	-3.9 ±8.8	49.9 ±10.9
270 Ma	16	51.1	157.4	3.6	11	38.1	239.6	7.4	15	21.7	117.9	7.8	5.4 ± 6.3	43.4 ±6.4	-6.4 ±7.9	99.7 ±8.0

Supplementary Table 1. The apparent rotation and poleward displacement of the Hronic Unit (48.9°N, 19.4°E) with respect to stable Europe and Africa (Torsvik et al., 2012) based on Debiche and Watson (1995), Enkin (2003b).

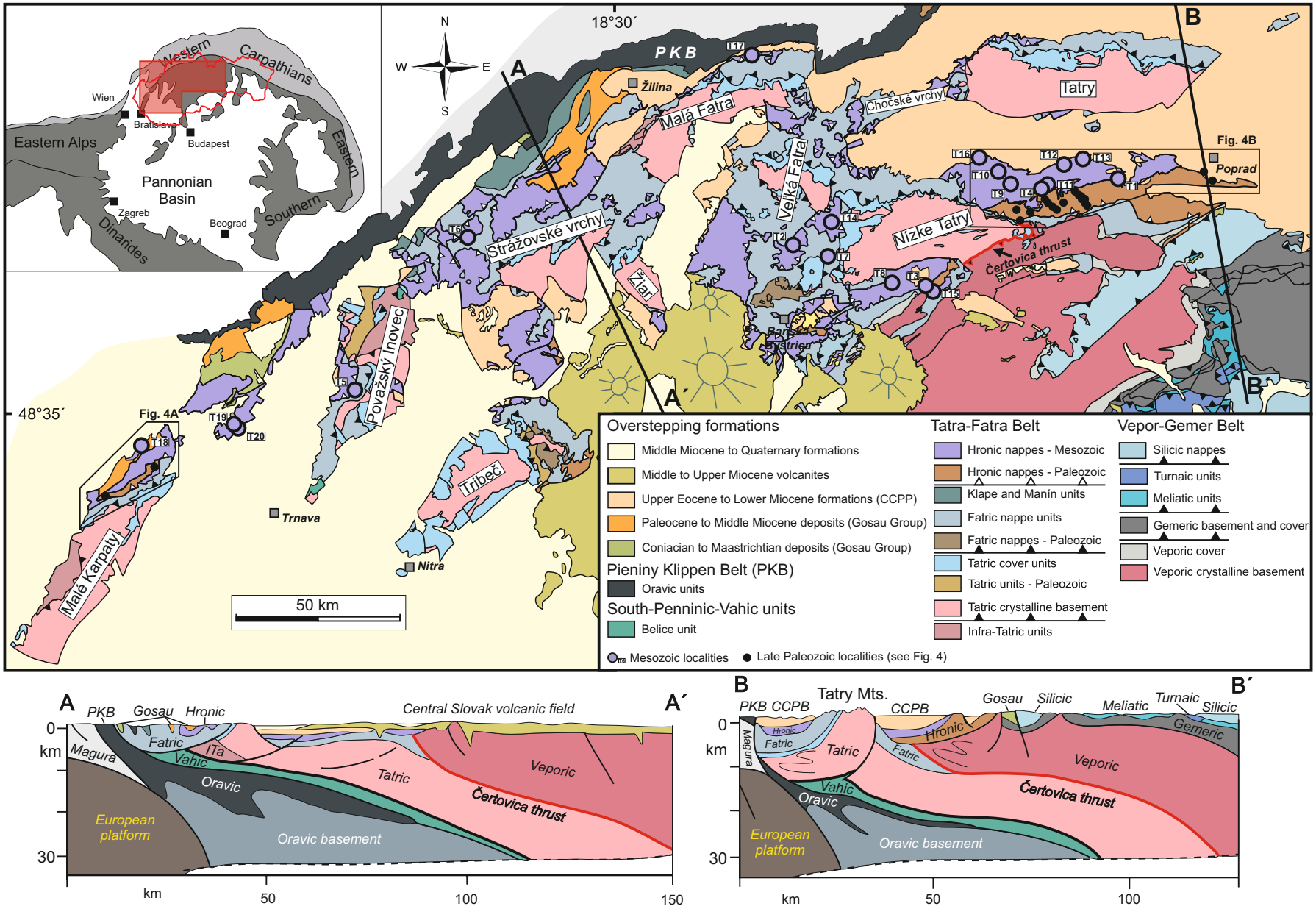

Fig. 1: Geological sketch map with sampling localities (based on Lexa et al., 2000; Bezák et al., 2004; Plašienka 2018).

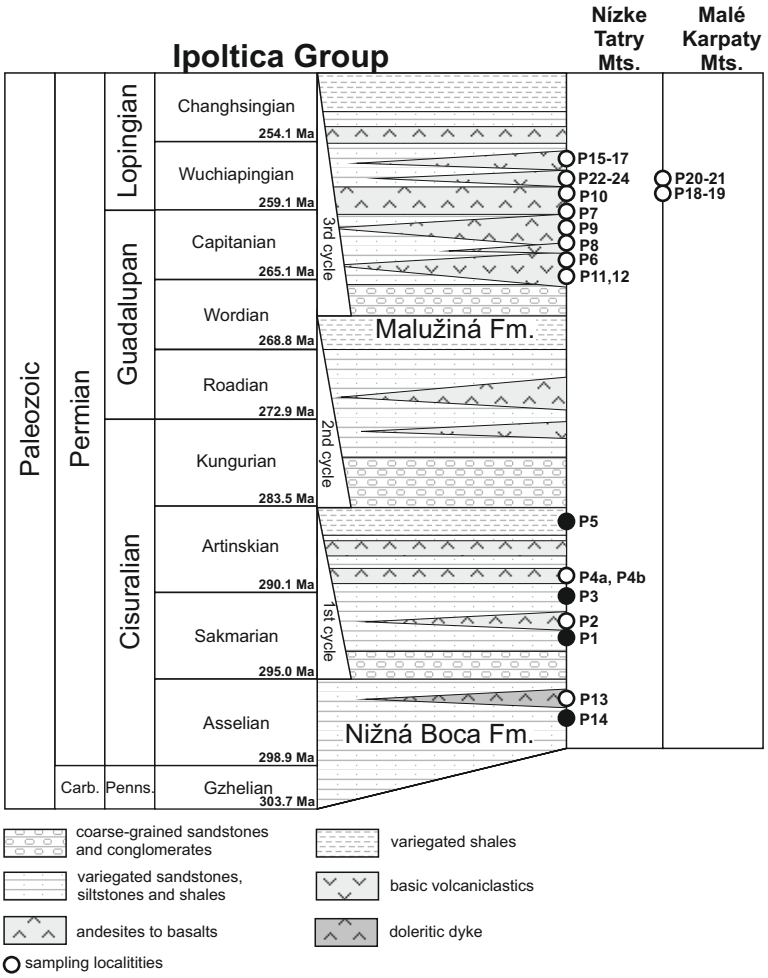

Fig. 2. Litostratigraphic column of the Late Paleozoic Ipoltica Group of the Hronic Unit with the position of sampling localities (based on Vozárová and Vozár, 1981; 1988; Vozárová et al., 2018). White circles (black dots) represent volcanic rocks (red sediments).

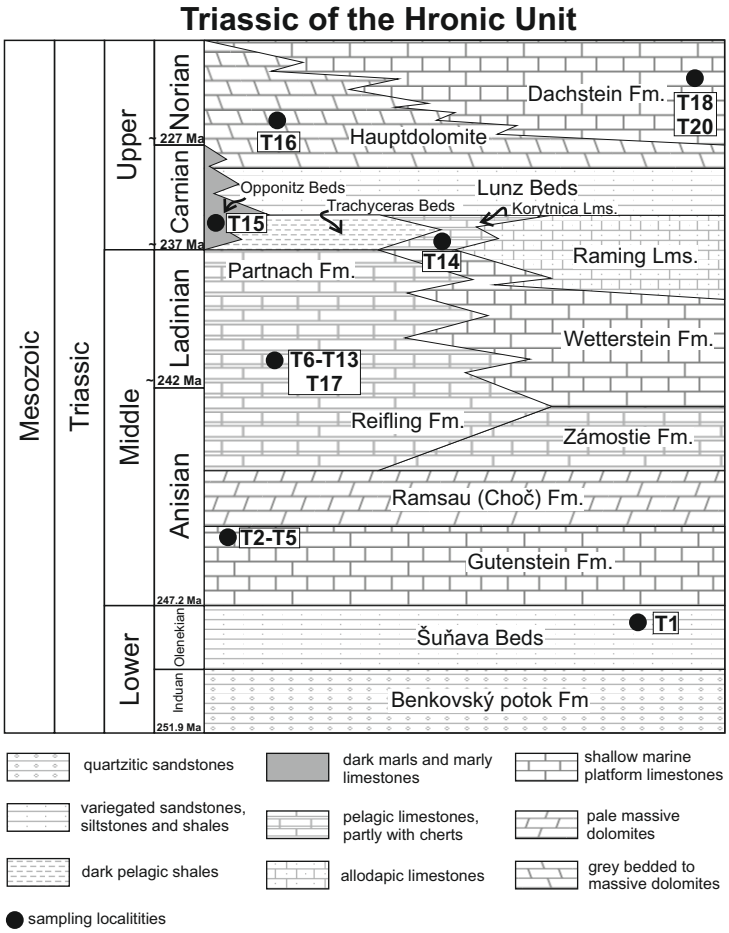

Fig. 3. Litostratigraphic column of the Triassic sequence of the Hronic Unit with the position of sampling localities (according to Havrila, 2011).

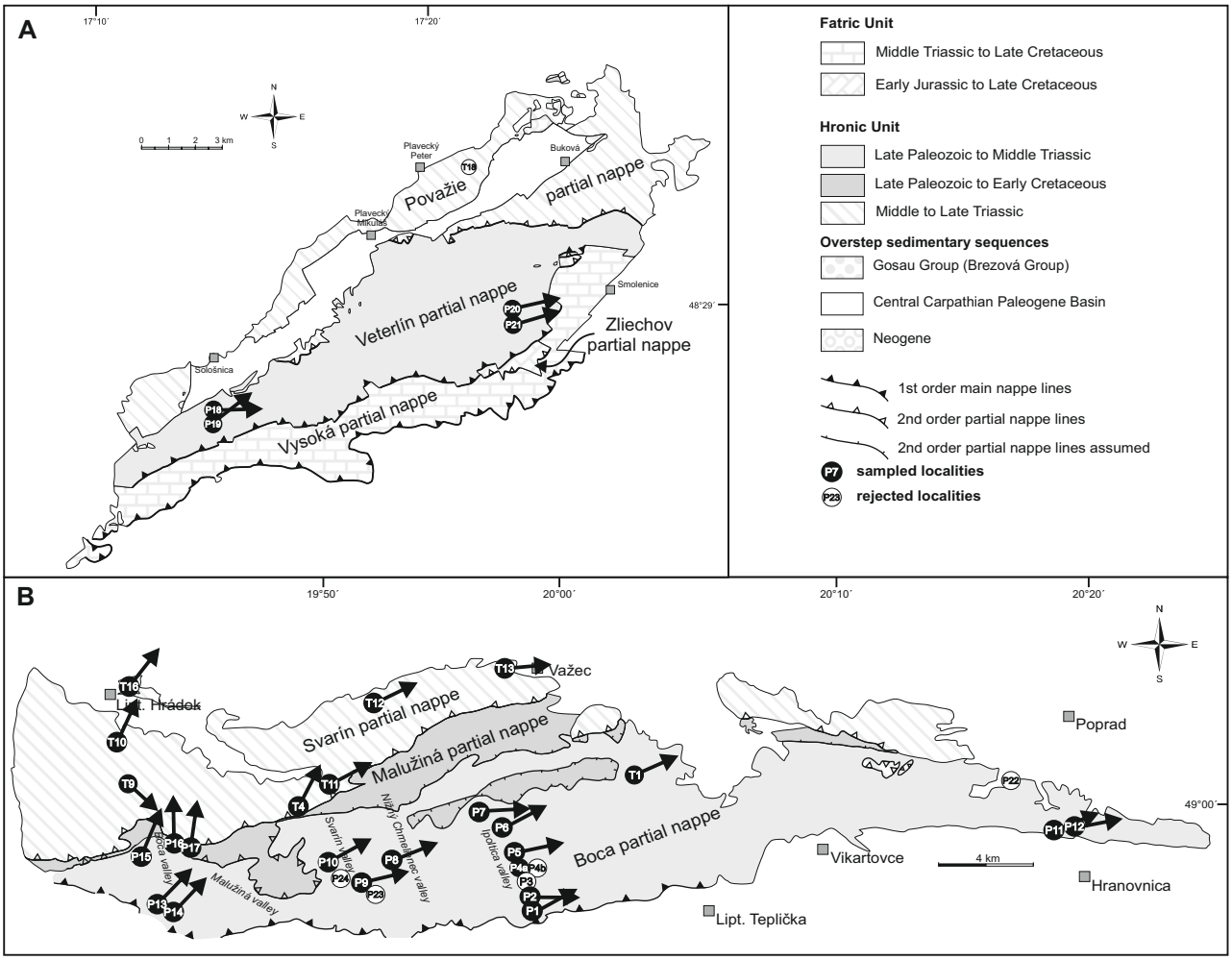

Fig. 4. Geological sketch maps of the study areas in the Malé Karpaty Mts. (A), and in the Nízke Tatry Mts. (B) with the sampling localities and paleodeclinations (based on Polák et al., 2011; Biely et al., 1992; Bezák et al., 2004). For the position of the study areas see Fig. 1.

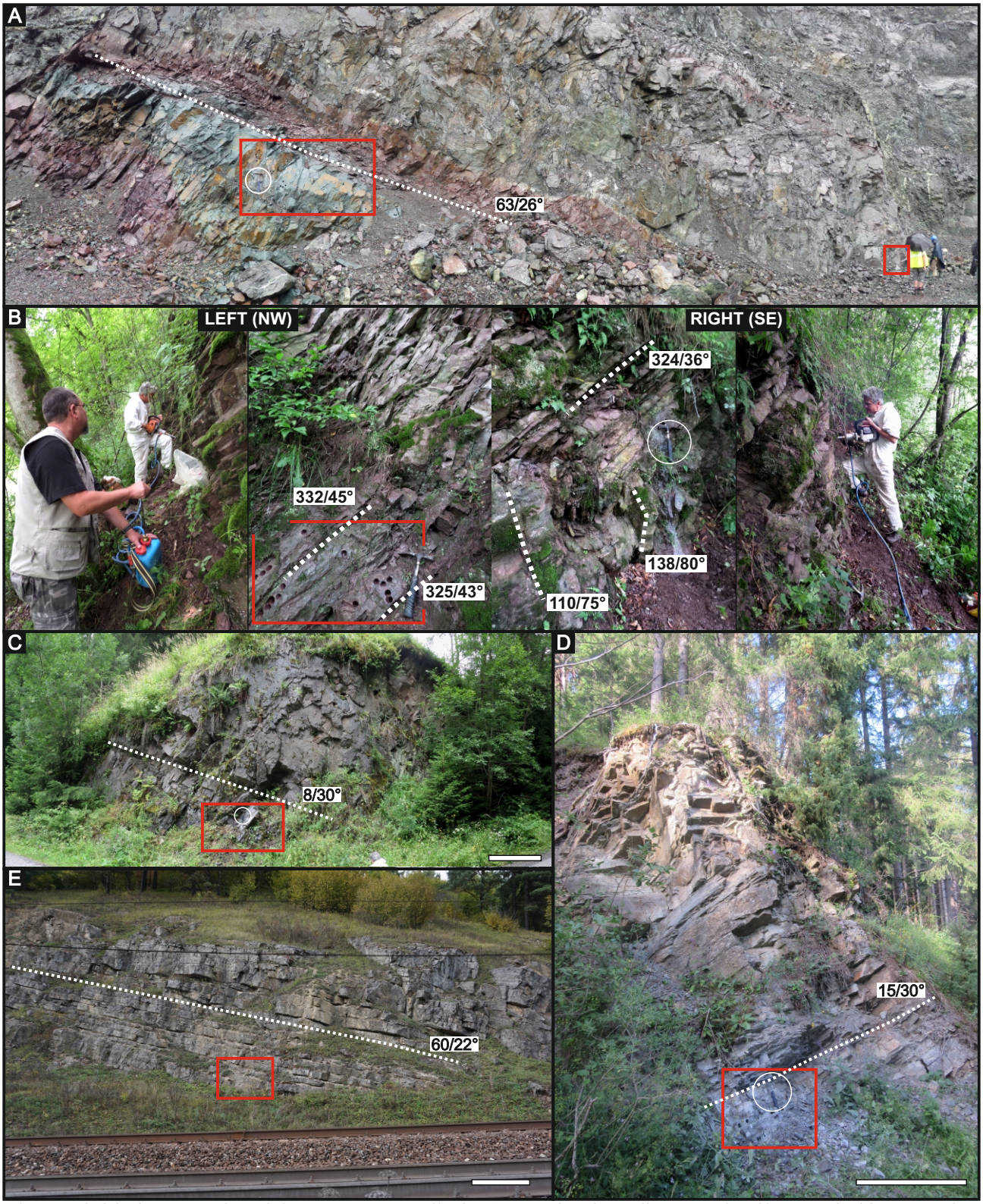

Fig. 5. Field photographs of the outcrops studied. A) Permian lava flows and tuffs sampled in Kvetnica quarry, locality P11; B) Permian red shales, locality P16; C) Permian lava flows exposed at locality P7; D) Lower Triassic variegated shales and sandstones at locality T1; E) Outcrop of the Middle Triassic Reifling limestones, a railway cut at locality T13. Red rectangles show the position of the sampling beds. Bedding planes or lava flow contacts are marked whith the white dotted lines. Hammer in the white circles is 33 cm long. White bars in C, D, E represent 1 m.

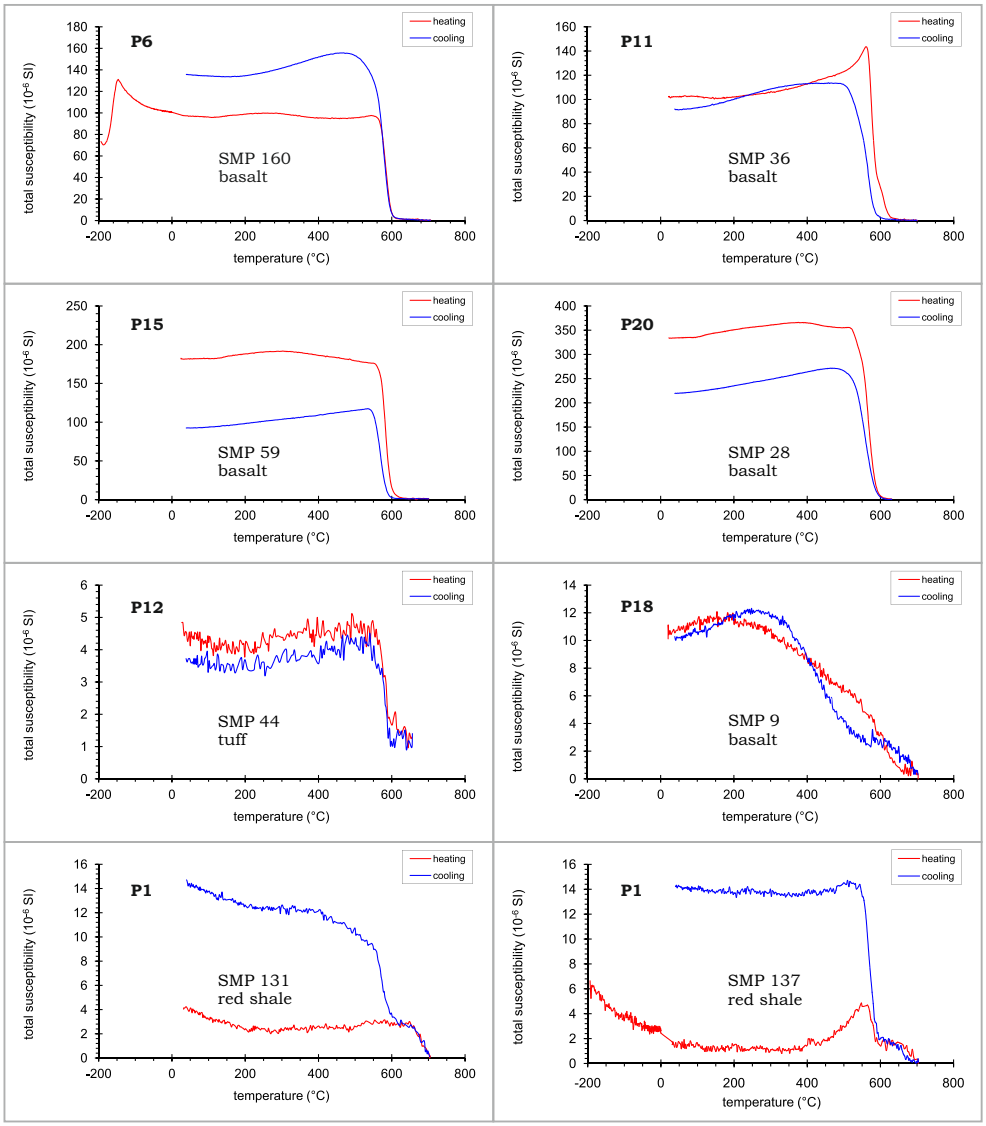

Fig. 6. Identification of magnetic minerals in the Permian rocks of the Ipoltica Group based on low field susceptibility versus temperature curves.

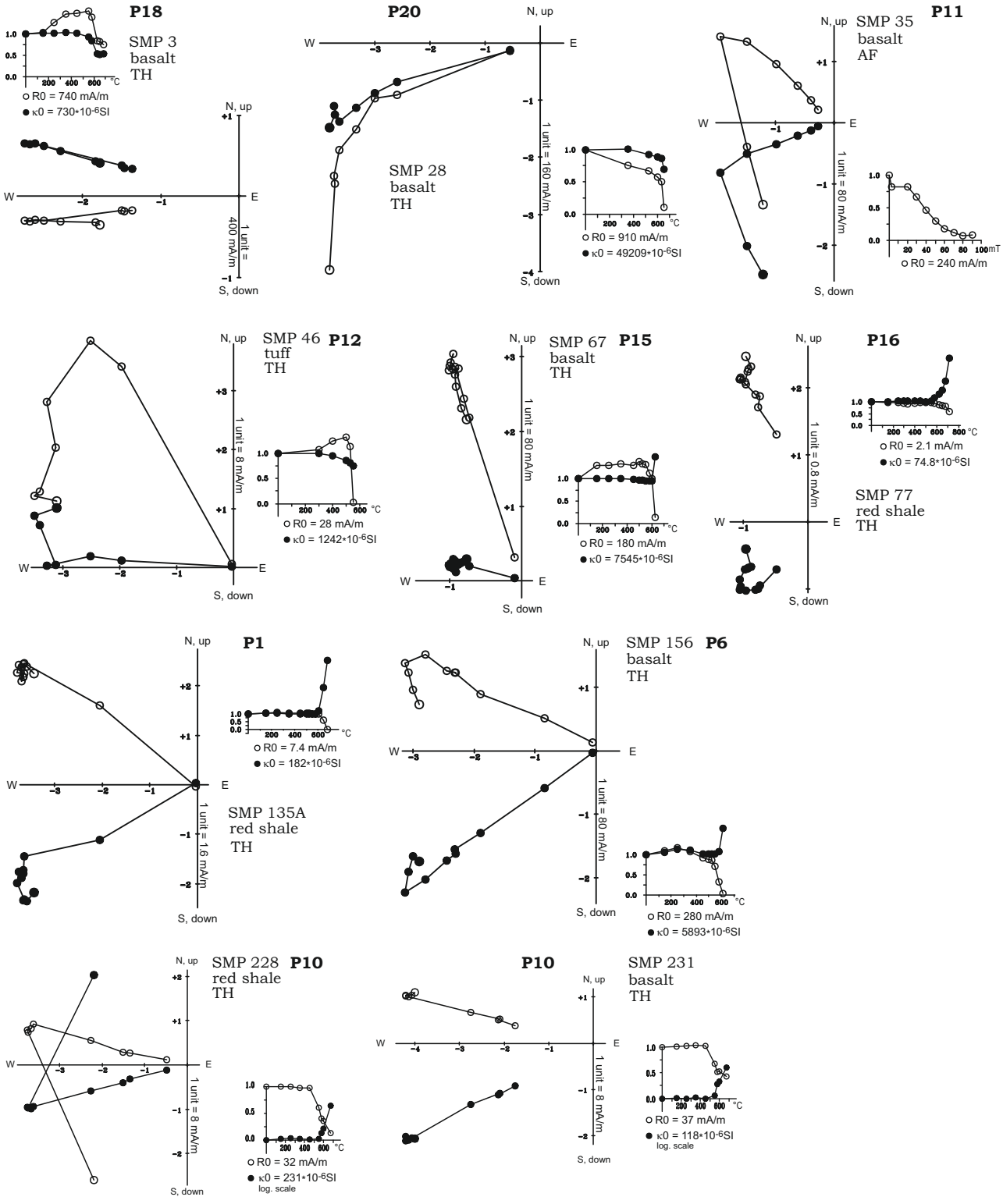

Fig. 7. Typical demagnetization curves for the Permian rocks of the Ipoltica Group. Key: Zijderveld diagrams are in the geographic system and are accompanied by intensity (circles) versus demagnetizing field diagrams, when the method of demagnetization is AF, and by NRM intensity (circles)/susceptibility (dots) versus temperature diagrams, when the method of demagnetization is thermal. In the Zijderveld diagrams full dots are the projections of the NRM vector onto the horizontal, circles into the vertical.

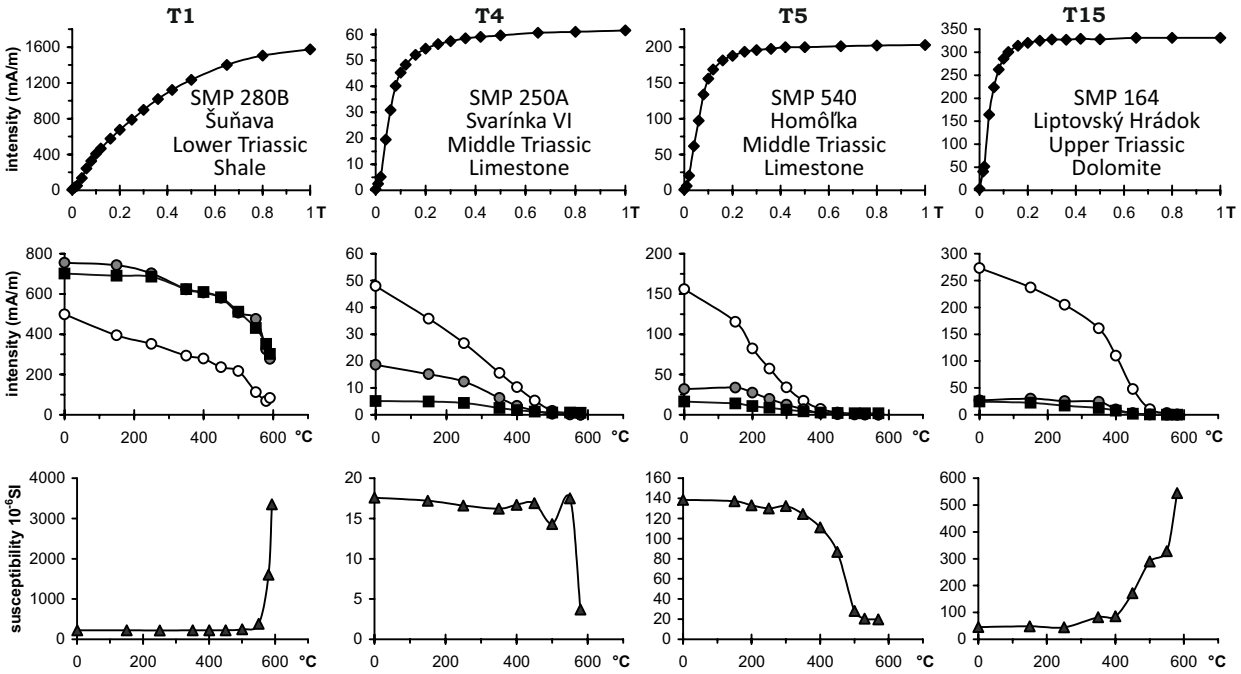

Fig. 8. Identification of magnetic minerals in the Triassic rocks of the Hronic Unit. Examples of the IRM acquisition (uppermost row), behaviour of the 3-component IRM (middle row) and the magnetic susceptibility (lowermost row) on stepwise thermal demagnetization. Key to the 3-component IRM: soft (circles), medium hard (dots) and hard (triangles) component, acquired in 0.12, 0.36 and 1.0 T fields, respectively.

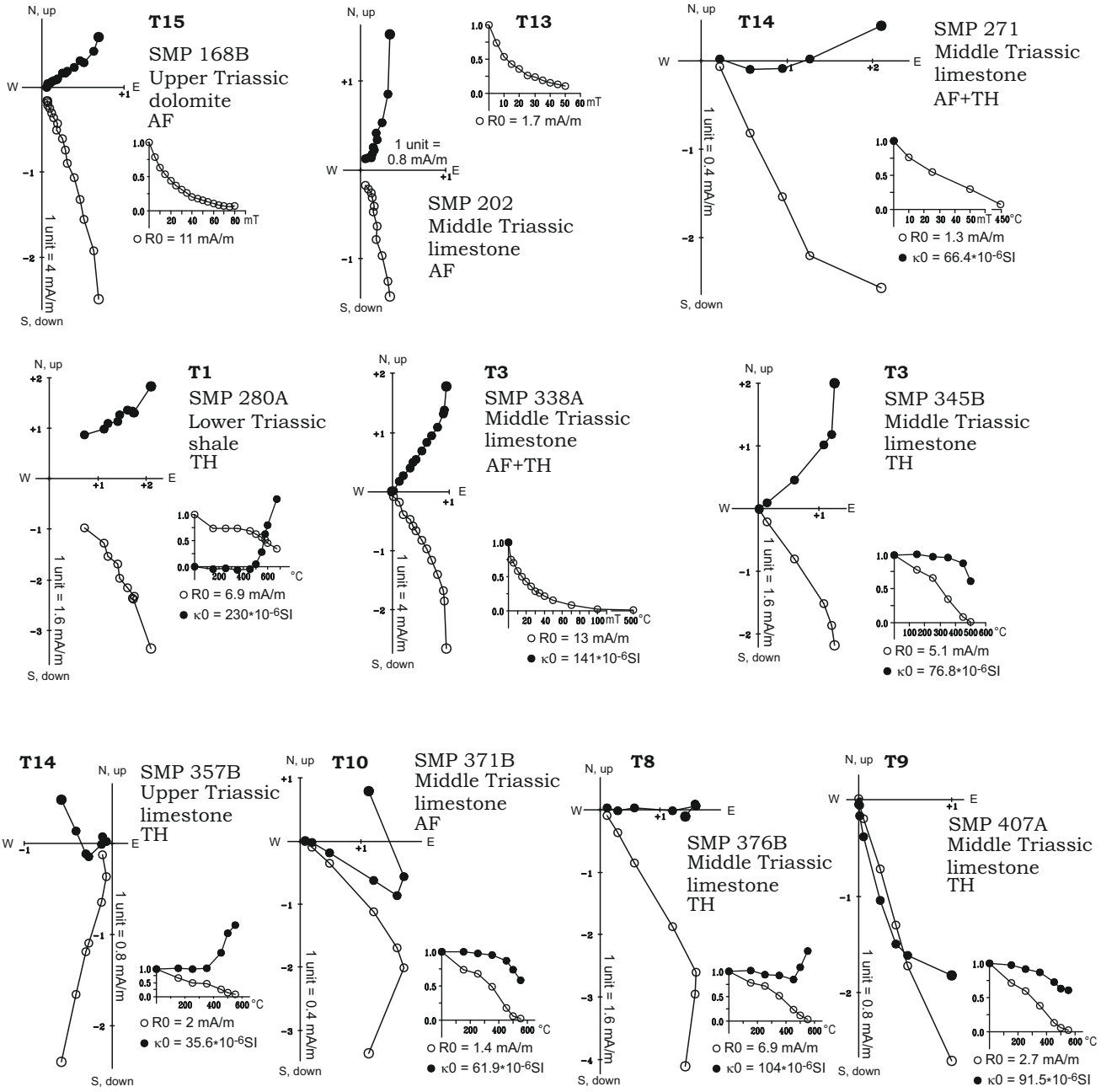

Fig. 9. Typical demagnetization curves for the Triassic rocks of the Hronic Unit. Key: as for Fig. 7 except locality T1 where the NRM intensity (circles)/susceptibility (dots) versus temperature diagrams are shown in the logarithmic scale because of dramatic susceptibility increase.

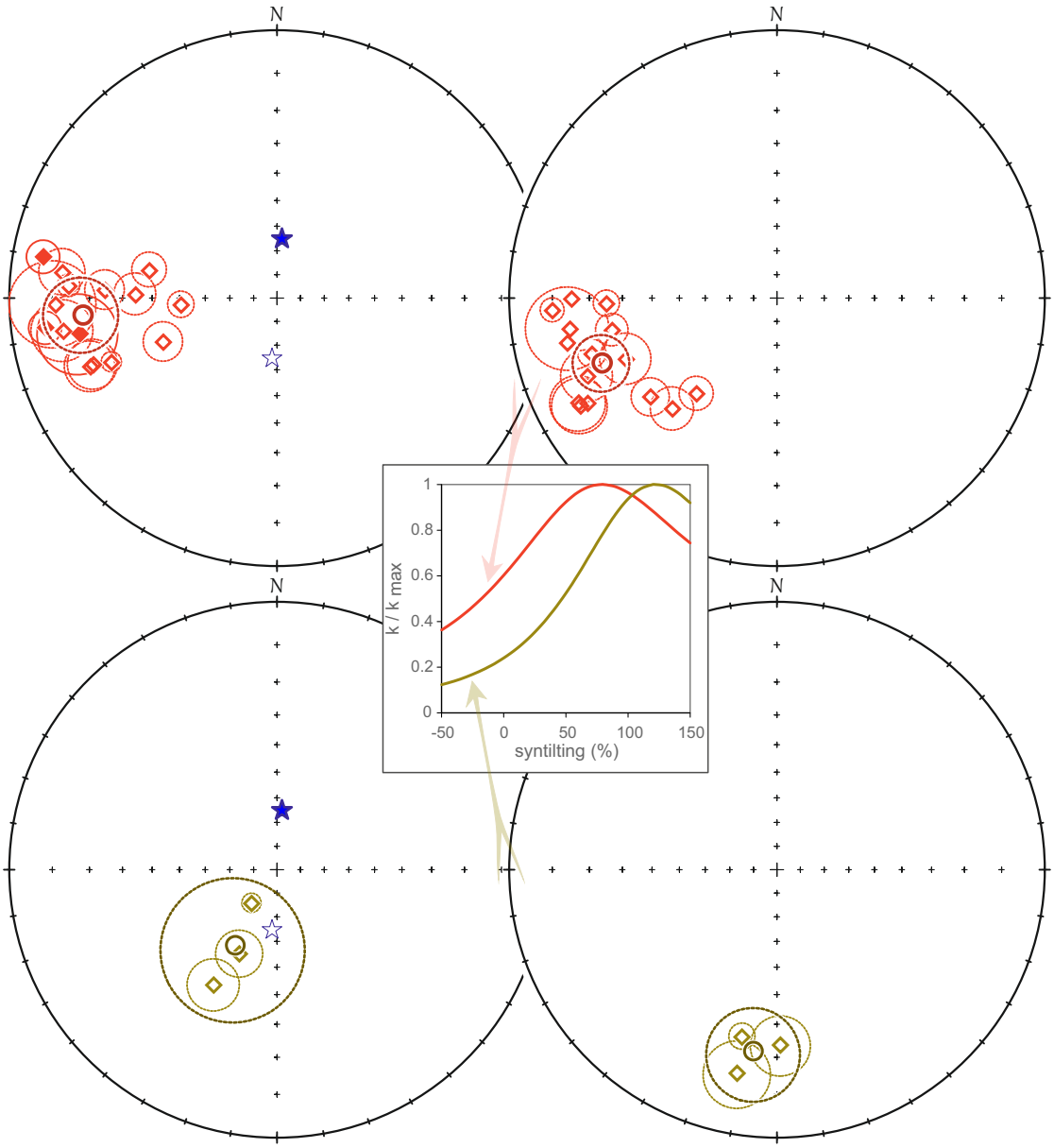

Fig. 10. Tilt test for the Permian rocks of the Hronic Unit without Malužiná partial nappe (upper row) and for the Malužiná partial nappe (lower row). Locality paleomagnetic mean directions with α_{95} are shown before (left side) and after (right side) tilt corrections. Stereographic projections, full/empty symbols = vectors pointing downwards/upwards. Stars represent the present day geomagnetic dipole field at the sampling area. Between the left and right diagrams the result of the stepwise untilting is plotted.

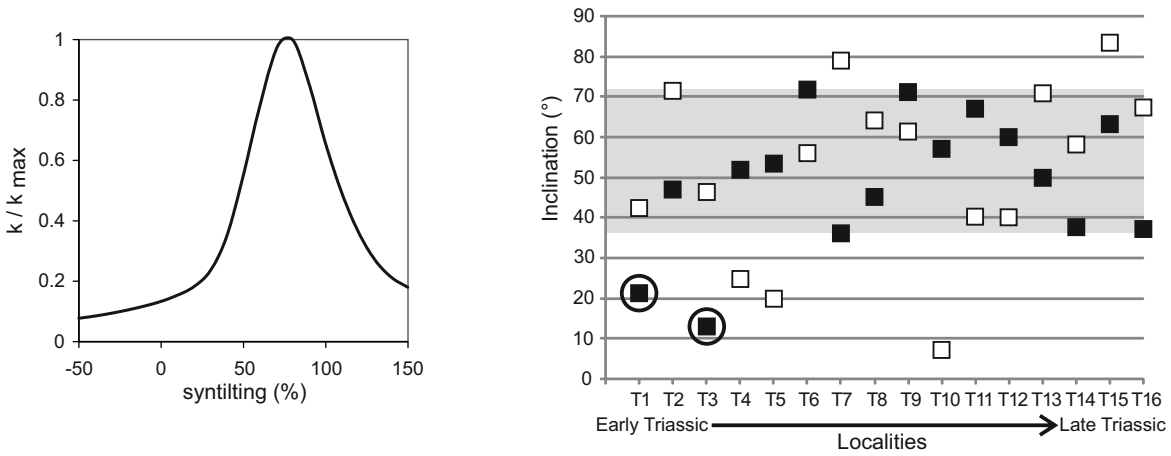

Fig. 11. Inclination-only test for Triassic rocks of the Hronic Unit. White (black) symbols represent inclinations before (after) tectonic correction. Localities in circles yield postfolding magnetizations (T1, T3).

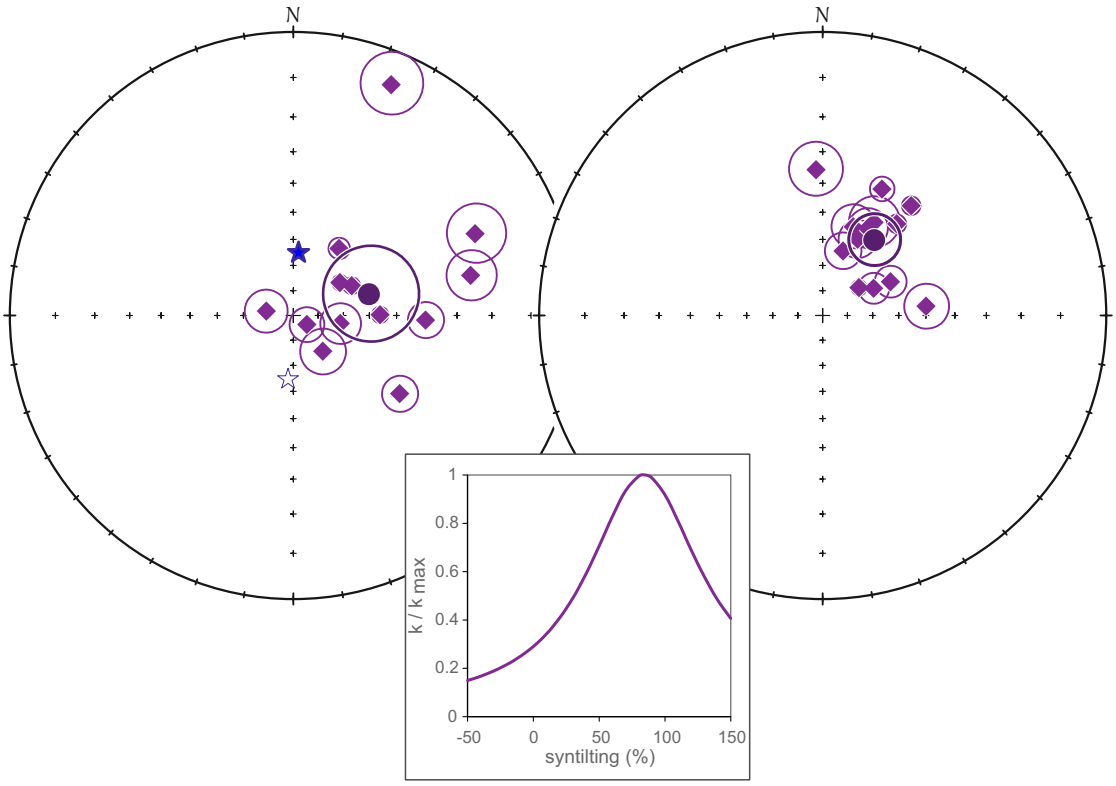

Fig. 12. Tilt test for the Triassic rocks of the Hronic Unit. Locality paleomagnetic mean directions with α_{95} are shown before (left side) and after (right side) tilt corrections. Stereographic projections, all vectors are pointing downwards. Stars represent the present day geomagnetic dipole field at the sampling area. Between the left and right diagrams the result of the stepwise untilting is plotted.

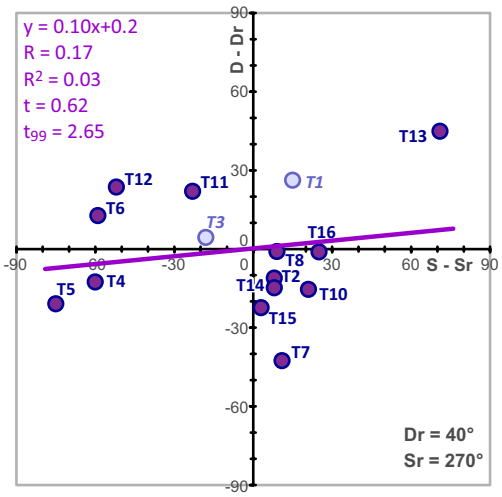

Fig. 13. Declination deviations relative to the fold axes deviations (method proposed by Schwartz and Van der Voo,1983 and successively applied by several authors, e.g. Speranza et al., 1997). Sr corresponds to the general W-E trend of the Hronic Unit, S is the strike measured at the respective localities. The overall-mean paleomagentic declination is Dr, D is the observed locality mean declination. The slope of the regression line does not differ significantly from zero slope, since the t test for the line is 0.62, which is much smaller than the critical value ($t_{99} = 2.65$) at 99% significance level.

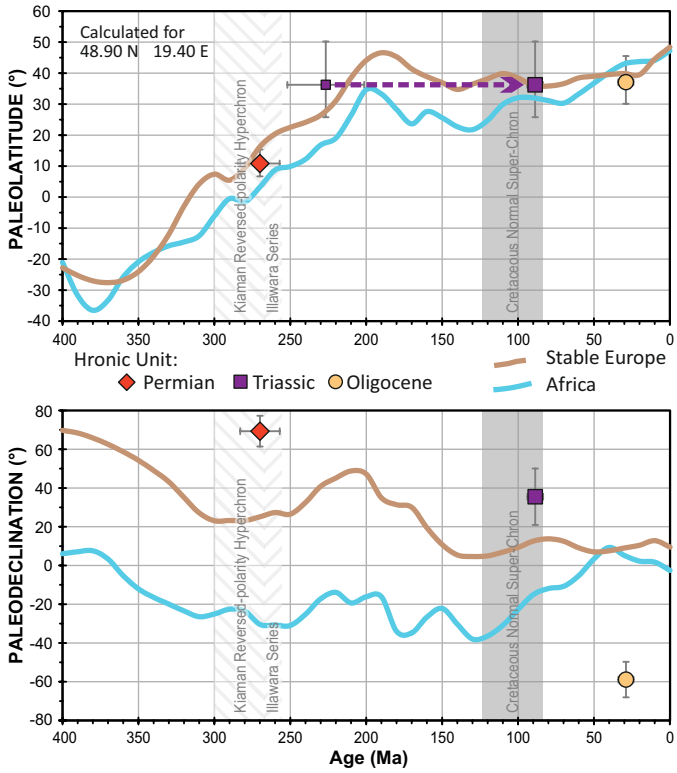

Fig. 14. Comparison of paleolatitudes and paleodeclinations for the Hronic Unit with those expected in an African and a stable European framework calculated from the APWP by Torsvik et al., (2012). All data are recalculated for a reference location 48.9°N, 19.4°E. Cretaceous Normal Super-Chron, Kiaman Reversed-polarity Hyperchron and the mostly reversed polarity part of Illawara Series are indicated by shaded intervals. All data for the Hronic Unit are from the present study, except those for the Oligocene which are from Márton et al., 2009, 2016). All calculations are based on Butler (1992).

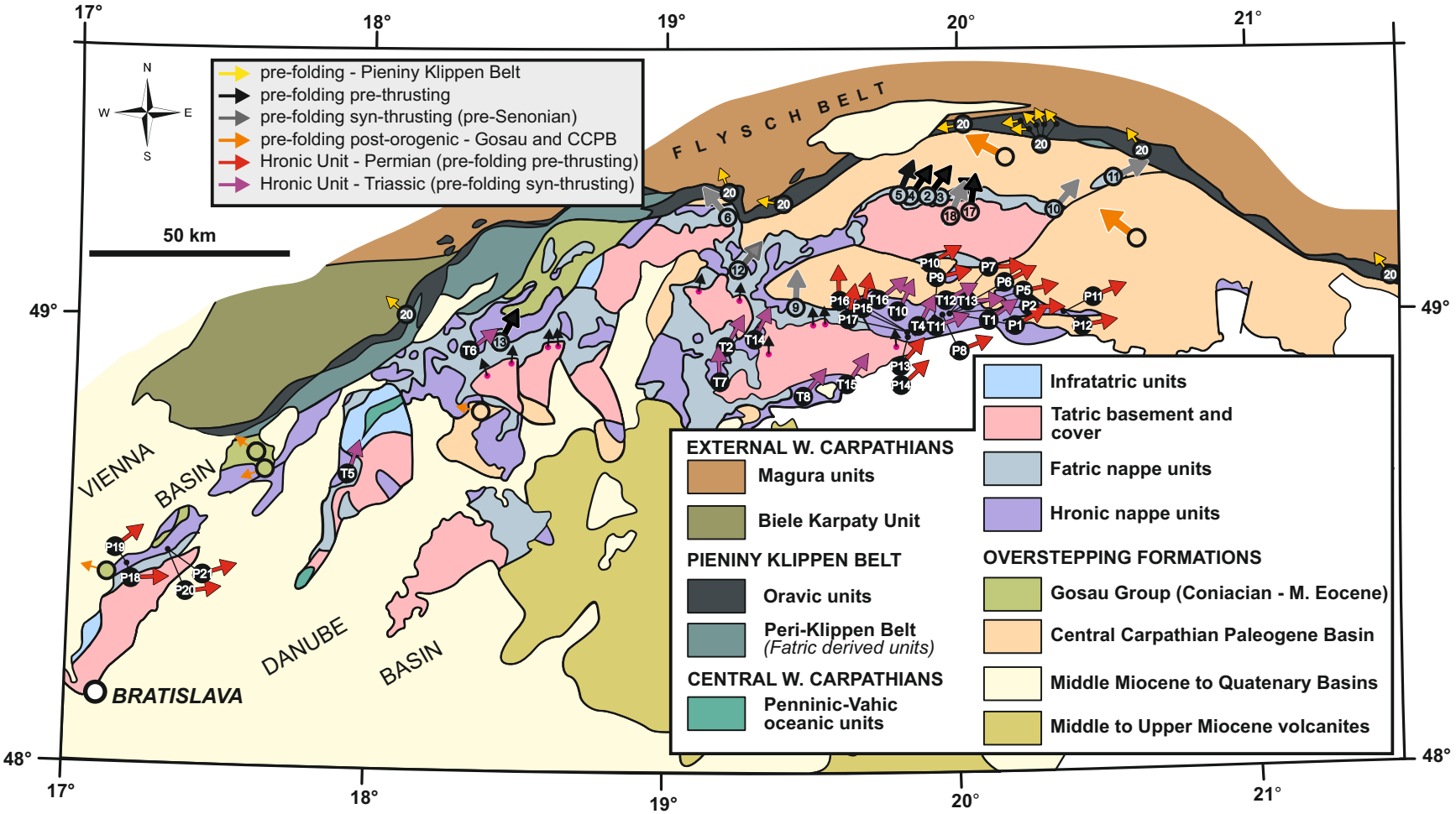

Fig. 15. Geological sketch map with distribution of paleomagnetic declinations for tectonic units of the Central Western Carpathians (map slightly modified after Plašienka, 2003; 2012). Red and purple arrows refer to our new results (see also Tab. 1, 2, Fig. 1, 4, present paper). Coloured circles are the locations from which the paleomagnetic results were published as the means for more than one sampling localities of similar age, accompanied arrows are black (positive fold test) or grey (exclusively N polarity), when the direction is interpreted as Late Cretaceous but pre-Senonian age and numbers correspond to items in Tables 1 and 2 for Mesozoic and Cenozoic rocks respectively in the overview by Márton et al., (2016). Green and yellow, not numbered circles with arrows are for Gosau Group and CCPB sediments from the same overview. Short black arrows are locality mean directions obtained for Lower Triassic sandstones of the Tatric cover Unit interpreted as primary (Szaniawski et al., 2020).